Effect of Mixture Properties and Testing Protocol on Moisture Susceptibility of Asphalt Mixtures

by

Kristoffer George Leatherman

A thesis submitted to the Graduate Faculty of
Auburn University
in partial fulfillment of the
requirements for the Degree of
Master of Science

Auburn, Alabama
August 4, 2012

Approved by

Randy West, Chair, Director of The National Center for Asphalt Technology (NCAT)
Michael Heitzman, Assistant Director & Senior Researcher (NCAT)
David Timm, Brasfield & Gorrie Professor of Civil Engineering
Buzz Powell, Assistant Director & Test Track Manager (NCAT)
Richard Willis, Lead Researcher (NCAT)
Nam Tran, Lead Researcher (NCAT)

Abstract

While cracking and rutting are the most prevalent distresses for asphalt mixtures, moisture susceptibility of asphalt mixtures which can lead to distresses such as raveling, loss of adhesion, and stripping is a commonly addressed concern in the mixture design procedure. As the industry shifts toward the use of warm mix asphalt (WMA) technology from the traditional hot mix asphalt (HMA) technology there has been increased concern regarding the performance of WMA technology in regards to moisture susceptibility. This concern is primarily driven by the decrease in required production temperatures of the asphalt mixtures which may result in aggregates that have not been dried thoroughly prior to being coated with asphalt binder.

In this report, 26 mixtures used for the 2009 National Center for Asphalt Technology (NCAT) Test Track and 61 mixtures evaluated for the National Cooperative Highway Research Program (NCHRP) 9-47A research projects were evaluated for their resistance to moisture damage using the most common laboratory tests for assessing such damage: AASHTO T 283 which results in a tensile strength ratio (TSR) and AASHTO T 324 Hamburg Wheel Tracking Device (HWTD) resulting in the stripping inflection point (SIP). In addition to WMA moisture susceptibility performance, the acceptability of the standard test protocols for moisture testing of asphalt mixtures were evaluated by comparing laboratory performance thresholds to the field performance of the mixtures.

As a result of this study, it was determined that there was no statistical difference between field compacted specimens versus laboratory reheated specimens for TSR and HWTD

results. WMA consistently showed statistically lower TSR and SIP compared to HMA control mixtures. The current specification criteria for HWTD may need to be adjusted assessing moisture susceptibility of WMA since several mixtures failed in the lab but showed good performance in the field. Statistical analysis also showed air voids consistently played a significant role in explaining the variability of the data. Finally, the change in texture data at the NCAT Test Track did not correlate well with moisture susceptibility testing results.

Acknowledgements

I would like to thank Dr. Richard Willis, Dr. Randy West, and Dr. Saeed Maghsoodloo for their extensive support in making this thesis possible. Additionally I would like to thank all of the members of my advisory committee for their support and guidance through this learning experience. Finally, I would like to offer my gratitude to my family and all others who helped by providing support from laboratory experiments to simple gestures and words of motivation.

Table of Contents

List of Tables

List of Figures

Chapter 1: Introduction

Moisture damage in asphalt pavements is one of the leading causes of pavement deterioration. This phenomenon instigates the stripping of asphalt mixture components resulting in rapid and severe damage to the pavement. According to a survey by the Colorado Department of Transportation conducted in 2002 which included 50 state departments of transportation, 3 FHWA Federal Land offices, the District of Columbia, and 1 Canadian province, 82 percent indicated that moisture damage to pavements under their jurisdiction constituted a problem significant enough to specify a treatment to mitigate the problem (1). While this is not a newly discovered issue, the increased use of warm mix asphalt (WMA) has raised questions regarding moisture susceptibility related to WMA treatments due to reduction of production temperatures.

1.1 Objectives

The primary objective of this study was to determine if there were significant differences in moisture susceptibility of WMA and hot mix asphalt (HMA) mixtures. Additionally, this study sought to determine whether significant differences in moisture sensitivity testing results occurred from the practice of compacting specimens in the field without reheating versus compacting specimens in a lab from reheated asphalt mixtures. Finally, data were analyzed to determine which mixture properties had the greatest influence on TSR and HWTD results.

1.2 Scope of Work

By using available resources, this study consisted of the fabrication and testing of multiple HMA and WMA mixtures for moisture susceptibility through the use of AASHTO T 283 and AASHTO T 324 testing specifications. Additionally, data from several projects were compiled and analyzed in conjunction with the initial data using various statistical techniques. Next, statistical models were developed to assess which mixture properties played the most

important role in the resulting moisture susceptibility criteria i.e. TSR and SIP values. Finally, texture data from the 2009 NCAT Test Track cycle were evaluated to determine whether a change in texture correlated with physical stripping of surface mixtures.

1.3 Thesis Organization

This thesis is divided into nine chapters. Chapter 1 covers the introduction, thesis objectives, scope of work, and overall organization of the document structure. Chapter 2 discusses the problems related with moisture damage in asphalt pavements by reviewing theories presented in the literature. Chapter 3 introduces the materials and paving projects utilized for the subsequent analyses. Chapter 4 details the testing methodology for obtaining the indirect tensile strength data along with various analyses comparing the results and fabrication techniques. Chapter 5 covers HWTD methodology and subsequent analyses of the resulting data including variations between specimens fabricated at paving project locations and those fabricated using reheated mix in a laboratory setting. Chapter 6 discusses similarities and differences between the two most popular moisture damage tests for asphalt pavements, AASHTO T 283 and AASHTO T 324. Chapter 7 covers the development of statistical models used to determine which mixture properties have the greatest influence on the final moisture damage criteria. Chapter 8 contains information regarding the change in texture data from the 2009 cycle at the NCAT Test Track and attempts to correlate the results with moisture damage of corresponding pavement sections. Lastly, Chapter 9 discusses the conclusions from this project in addition to recommendations based on the findings of this report.

Chapter 2: Literature Review

By reviewing literature related to moisture damage, it is quickly understood that there are multiple factors at work when evaluating pavement deterioration caused by moisture. In this chapter several theories and mechanisms contributing to moisture damage are discussed. These theories were developed in order to gain a better understanding of the problem and attempt to address the issue at the most fundamental levels. By understanding the problem in detail, it may be possible to develop methods and practices which prevent or minimize the negative effects of moisture in asphalt pavements. Additionally, several conditioning and testing methods are discussed in order to evaluate moisture damage in a laboratory setting.

2.1 Moisture Damage

Moisture damage, often referred to as stripping, in HMA is the phenomenon in which water compromises the interface between the aggregate and the asphalt resulting in a lack of cohesion between the two mixture components. As a result, pavements can experience distresses such as premature cracking which significantly reduces the service life of the structure. This problem is typically characterized by either a loss of adhesion or a loss of cohesion. The former is the result of the presence of water between the aggregate and the binder which causes stripping to occur, and the latter is the result of water softening the binder causing a decreased bond between the aggregate and the binder (2). Many factors affect this process including aggregate properties, asphalt concrete mixture characteristics, binder properties, environmental factors, and production/construction practices (2).

2.2 Adhesion

A fundamental attribute of asphalt concrete is the ability of the aggregate to bond to the asphalt binder through adhesion. Adhesion is defined as the force of attraction between unlike molecules that makes bodies stick together (3). There are several theories which attempt to explain adhesion including: mechanical theory, chemical reaction theory, surface energy theory, and molecular orientation theory (2). While none of these theories fully explain the actual mechanism by which adhesion works, each theory provides a different perspective on the phenomenon. Below a brief overview of each theory is presented.

2.2.1 Mechanical Theory

Mechanical theory states the bond between the aggregate and the binder is created by a mechanical lock occurring between the two mixture components. This locking action is assumed to be derived from the cohesion in the binder and interlocking properties of the aggregate particles (4). Several factors are suggested to be participatory in this action including surface texture, porosity, surface coatings on the aggregate, surface area, and particle size(2). Roughness is thought to play a role in that the asphalt cement is forced into the pores and irregularities of the aggregate surface to provide a stronger mechanical interlock. Greater porosity and absorption capacity are generally associated with improved adhesion; however, the pore size may be more significant than the total volume of pores in the aggregate. Dust and moisture or other elements coated on the aggregate tend to decrease the bond between the asphalt cement and the aggregate. Finally, particle size has been shown to play an important role as finer material has more surface area and thus requires more asphalt cement to completely coat the aggregates. As a result, mixtures with more fines tend to strip more readily as more asphalt cement is required for complete particle coating which can often lead to stability issues (2).

2.2.2 Chemical Reaction Theory

Chemical reaction theory makes a connection between the acidity of the aggregate and bond strength of the resulting asphalt concrete mixture. It has been noted that aggregates with higher acidity have weaker bonding than aggregates with more basic characteristics. This is because highly acidic aggregates, those which generally exhibit high silica content, are typically considered hydrophilic and have an attraction to water (4). Such aggregates include quartzite, sandstone, and granite though quartzite has been shown to be less susceptible to stripping than most basic aggregates, those with low silica content and high $CaCO_3$ content(4),(6). Some examples of basic aggregates, which are considered to be hydrophobic, include marble, limestone, and basalt. Based on this information, it has been suggested that additives which reduce the acidity of aggregates might improve bonding and decrease the mixtures potential for stripping (2).

2.2.3 Surface Energy Theory

Surface free energy of a material is defined as the amount of work required to create a unit area of a new surface of that specific material in a vacuum (7). A change in energy takes place when asphalt wets an aggregate surface. The energy change, referred to as adhesion tension, depends upon the closeness of contact and mutual affinity of the asphalt cement and aggregate. With data supporting higher adhesion tension in water than asphalt, the water will displace the asphalt if present at the interface between the asphalt binder and the aggregate (2). Tests were performed to measure the surface energy components of asphalt binders and aggregates including unmodified and modified binders. The typical range of values for the surface energy components, work of cohesion and adhesion, and energy parameters with different aggregates were determined and reported to serve as a guideline for future

measurements. The energy parameters were then computed using the surface energy components of the asphalt binders and aggregates and used as a screening tool to select optimum combinations of asphalt binders and aggregates. The study also included the use of liquid anti-strip agents which typically reduced the non-polar component of the surface free energy which in turn reduced the work of cohesion of the asphalt binders. The addition was shown to indirectly improve the fracture resistance by promoting better adhesion between the fines and the binder during the mixing and compaction process. While using anti-strip agents is already known to promote better adhesion, this study concluded that using the surface energy theory was a successful tool to evaluate this observation (7).

2.2.4 Molecular Orientation Theory

Molecular orientation theory states that when asphalt binder comes into contact with an aggregate surface, the molecules in the asphalt orient themselves so as to satisfy the energy demands of the aggregate. Considering asphalt molecules are generally nonpolar and water molecules are dipolar, it is suggested that the water molecules more readily satisfy the energy demands of the aggregate. Even though there are cases where binders may contain dipolar molecules which have a greater energy demand for aggregates, this effect may not be significant as dipolar molecules are not predominant in asphalt binder (1).

2.3 Stripping Mechanisms

Hammons et al. (8) states there are five possible mechanisms of stripping in asphalt concrete mixtures including detachment, displacement, spontaneous emulsification, pore pressure, and hydraulic scouring. It is noted that the detachment and displacement mechanisms do not require moisture to be present for these phenomenon to occur; however, for the purpose of discussion, they will be mentioned in association with moisture. In addition to these five

mechanisms, an additional mechanism, film rupture, has been linked with moisture damage and will be discussed (3).

2.3.1 Detachment

Detachment is defined as the separation of asphalt from the aggregate surface by a thin layer of water with no obvious break in the asphalt film. This results in the asphalt film being peeled cleanly from the aggregate (3). Since asphalt binders are not impervious, water is able to permeate through the binder to the aggregate surface and cause the detachment (4).

2.3.2 Displacement

Similar to detachment, displacement results in the removal of the asphalt binder from the aggregate surface. However, this type of stripping results from a break in the binder whereas detachment occurs between the binder and the aggregate. The break may be caused by incomplete coating during mixing or from asphalt film rupture (3).

2.3.3 Spontaneous Emulsification

Evidence suggests that under traffic asphalt mixtures can react with free water to form an inverted emulsion of water droplets in the asphalt cement. This then strips the asphalt binder off the aggregate structure of the mixture (3),(4). Researchers have observed some anti-strip additives act as emulsifiers when they come into contact with water even though they initially help the asphalt form a better coating on the aggregate. Other studies have shown binders can recoat the aggregate structure when stored in a dry setting upon water evaporation (3).

2.3.4 Pore Pressure

Pavements with high air voids may contain interconnected voids in which water is free to move. Over time, traffic may further compact the mixture closing some of the voids and trapping

the water in the pavement. As traffic continues, the water builds up pore pressure to the point of stripping the asphalt from the aggregate (3). This stripping commonly occurs at asphalt layer interfaces where more interconnected voids exist. Mixtures typically disintegrate from the bottom upward starting in the binder layer and moving to the surface layer; however, there have been cases where disintegration has begun within a layer and proceeded in both directions (4).

2.3.5 Hydraulic Scouring

Hydraulic scouring typically occurs in surface courses which are saturated and subjected to traffic loadings. The wheel of the vehicle presses water into the pavement in front of the tires and the movement of the tire along the surface of the pavement results in suction pulling the water out behind the tires. While water moving through the pavement structure has been known to cause stripping, the damage can be inflated if dust is mixed with the water resulting in a more abrasive scrubbing mechanism on the surface of the asphalt covered aggregate (4).

2.3.6 Film Rupture

While this mechanism is not a direct cause of stripping, it is noted that it helps facilitate stripping. Rupture of the asphalt film on the aggregate particles is likely to occur under stresses of normal traffic or construction loads at the sharp edges and corners where the film is the thinnest (3),(4). It is also suggested that the breaks could be environmentally induced through freeze-thaw cycling (4). The presence of dust or other surface coatings on the aggregate can enhance the formation of blisters and pits which may lead to rupturing of the film (4).

2.4 Factors Contributing to Stripping

While there are several theories and mechanisms which attempt to explain how stripping physically manifests itself, there are several mix design and mix production factors that can impact moisture sensitivity. Hammons explains that some factors include inadequate asphalt

content, excessive dust coating on the course aggregate, and aggregate contaminated with unburned fuel upon going through the heating drum (7). Some other factors that may contribute to premature stripping include inadequate pavement drainage, inadequate compaction, the use of open-graded friction courses (OGFC) on top of HMA layers with high air voids, inadequately dried aggregate, weak and friable aggregates, specific aggregate type, and waterproofing membranes/seal coats that trap moisture within a pavement structure (10). A brief discussion of each of these factors is presented below.

2.4.1 Inadequate Asphalt Content and Excessive Dust Coating

Inadequate asphalt content in the mix may result in incomplete asphalt coating on the aggregates at the time of production/construction allowing the uncoated aggregates to absorb moisture (7). Additionally, an excessive amount of dust on the course aggregate can interfere with the adhesion between the aggregate surface and the asphalt binder. As the asphalt ages, the asphalt film surrounding the aggregate can crack and cause the aggregate to break free from the mixture (7). It is also noted that in the presence of water, dust coated particles strip readily as the dust creates pinholes in the coating which give water access to the aggregate surface (3).

2.4.2 Contaminated Aggregate

Aggregate contaminated with unburned fuel may inhibit adhesion between the asphalt and aggregate surface at the time of production. This can cause the aggregate and binder to displace relative to one another due to the lack of shear strength. This characteristic has been exhibited by HMA mixes produced using older drum mix plants when dirty fuel oils which were not preheated were used to dry aggregates (7). Due to advancements in asphalt production plants, this issue may not play as large a role as in previous years.

2.4.3 Inadequate Pavement Drainage

As water is a necessary ingredient for moisture induced damage, adequate pavement drainage is necessary to help prevent this problem. Kandhal reported case histories where the stripping was not a general phenomenon occurring on the entire project but rather a localized occurrence. These problems appeared in areas of the project which were over-saturated with water and/or water vapor due to inadequate subsurface drainage conditions 0. This often occurs when roads are widened with no consideration to increasing the subsurface drainage capacity 0.

2.4.4 Inadequate Compaction

According to Kandhal, inadequate compaction of the HMA mat is probably the most common construction issue responsible for premature stripping. While the typical maximum air void target for newly constructed pavements is 8%, some agencies do not exercise good compaction control which can lead to premature surface raveling as the mix does not possess adequate cohesion 0. Additionally, inadequate compaction leads to a mat which has a larger void structure. The mixture is then more permeable and, thus, more susceptible to stripping.

2.4.5 OGFC over High Air Void Pavements

Several states in the southeastern United States experienced stripping in the HMA course underlying open-graded asphalt friction course (OGFC) during the late 1970s 0. Some theories suggest that the OGFC layers retain moisture longer than traditional dense graded asphalt mixes and the water is forced into underlying layers by truck tires resulting in stripping action. To alleviate this issue, several states suspended the use of OGFC in the early 80's until later studies showed it is necessary for layers underneath OGFC mixtures to contain no more than 4-5% air voids to provide an impermeable base 0.

2.4.6 Inadequately Dried Aggregate

It is well known that aggregate with high residual moisture content and aggregates that absorb water readily will significantly increase the potential for stripping if not properly dried prior to production (3),0. Dry aggregates will improve the wettability and increase the adhesion between the aggregate surface and the binder; the increased temperature required to thoroughly dry the aggregate will also increase the wetting power of the asphalt by reducing the viscosity (3).

2.4.7 Weak and Friable Aggregate and Specific Aggregate Types

Weak aggregates have a tendency to break during compaction and heavy traffic loading. This, in turn, creates new aggregate surfaces which are not coated with binder. These new surfaces provide locations for moisture to saturate the aggregate initiating stripping in the mix 0. There is also information to suggest that the specific type of aggregate used in a mix may have significant contributions to moisture susceptibility. Some studies addressing this issue will be discussed in a later section.

2.4.8 Waterproof Membranes and Seal Coats

When the primary source of moisture in a pavement is from underneath the pavement structure and an adequate drainage system is not in place, sealing or placing a waterproof membrane between asphalt layers can be detrimental. Waterproofing membranes effectively trap the moisture in lower layers of the pavement structure causing significant vapor pressure and inducing an environment conducive to moisture damage in the lower levels of the pavement (3). For this reason, it is important to evaluate the current drainage ability of the pavement and major sources of moisture before sealing or placing a waterproofing membrane in a pavement structure.

2.5 Reducing Stripping Potential

Due to the many mechanisms and factors which contribute to moisture damage, pinpointing one method to prevent this distress is difficult to achieve. However, based on previously mentioned stripping mechanisms, there are several suggested practices which may aid in the reduction of stripping potential. Using clean quality dry aggregates which are not hydrophilic will help prevent moisture damage by developing a strong bond between the asphalt binder and the aggregate surface. It is also noted the asphalt mixture's resistance to moisture damage is related to the type of aggregate in the mix in addition to the asphalt composition (10). If possible, avoid paving in cool and wet weather conditions as this can lead to insufficient or poor compaction and have a pronounced influence on the susceptibility of the pavement to moisture damage (3). Ensure that the pavement has adequate subsurface drainage. Several case studies completed in Pennsylvania and California have shown that moisture held within the pavement can lead to accelerated damage (3).

2.5.1 Anti-strip Agents

Using anti-strip agents (ASA) is a popular method of preventing moisture damage. According to Anderson et al. (10), anti-strip agents are understood to act like chain molecules which attach themselves to the asphalt particles as well as the aggregate surface. The liquid agents are typically amine-based additives which interact with polar, viscosity building components to improve the bond between the aggregate surface and the asphalt binder (10),(11). Proper precautions should be taken when using liquid ASA as some are known to have offensive odors and even cause nausea. Additionally, care should be taken as some liquid anti-strip agents can have issues with the consistency of the asphalt cement as well as heat stability issues (12). This problem can start as soon as the component is exposed to any source of heat including the introduction to the tanker, transfer into plant storage tank, addition into the mixing drum, and

storage in the silos. Due to this issue, most chemical anti-stripping additives are classified as being "heat stable" by their manufacturers (2). Other anti-strip agents include mineral additives which are typically inorganic powders such as hydrated lime, portland cement, fly ash, flue dust, and others, with hydrated lime being one of the more widely used of the mineral additives (11).

2.5.1.1 Hydrated Lime Treatment

As previously mentioned, hydrated lime is widely used to aid in the prevention of moisture related damage in AC pavements. Hydrated lime is typically added to asphalt mixtures as an ASA either dry or in a slurry. Kim et al. (12) showed that the addition of lime both in dry form and in slurry form decreased the extent of moisture damage in HMA by performing HWTD and asphalt pavement analyzer (APA) testing. The primary problem with the addition of dry lime is holding the lime on the surface of the aggregate until it is coated with asphalt (2). Other issues with dry lime include the loss of lime due to gas flow and lime acting as mineral filler with portions combining with the liquid asphalt (2). It was also shown that introducing mineral filler into the mix provided comparable results to adding lime over the course of one freeze thaw (F-T) cycle using the AASHTO T283 test method. However, when subjecting the samples to six F-T cycles, the mineral filler performed poorly compared to the lime treated specimens which retained approximately 30-40% more strength than those without lime treatment (12).

Kennedy et al. (13) concluded that the most effective method of applying a lime ASA is in the slurry form. Stockpiling the lime treated aggregate additionally helped to reduce the moisture content of the coated aggregate prior to production, but was not required for "curing." Kennedy (13) also noted drawbacks to using lime slurry. The need for special equipment and controls, the necessity to remove the moisture from the aggregate prior to mixing with asphalt and the possibility of special handling to stockpile the treated aggregate were among the most

detrimental to using lime slurries. Having to remove additional water can increase fuel costs and decrease production rates; therefore, it is important to minimize the amount of water which has to be removed when the aggregate enters the dryer of the drum mixer (2).

2.6 Recognizing Moisture Damage in the Field

Moisture damage is difficult to recognize as it can be a precursor to other pavement distresses such as rutting, shoving, raveling, or cracking (11). The most common method used to identify stripping in the field is taking cores and splitting them to visually evaluate the stripping of the asphalt from aggregates 0. While cores are commonly removed from the pavement using water as a lubricant, this practice should be avoided so that the moisture content of the core can be determined.

Figure 1. Stripping After Core Removal (Pavementinteractive.org)

A study was performed by the Georgia Department of Transportation between 2004 and 2005 to determine if nondestructive testing methods could be used to detect whether or not in place asphalt pavements contained stripping. Several tests were performed in the field including

air-coupled ground penetrating radar (GPR), infrared thermography, digital surface distress survey, rutting (transverse profile), roughness (longitudinal profile in the wheel paths, falling weight deflectometer (FWD), and seismic measurements. It was determined that forward-calculated HMA stiffness values from FWD deflection basins were not sensitive to stripping in thin HMA layers when the layers were located between thicker layers without stripping. Thermal anomalies were not found to be reliable indicators of stripping in thick HMA pavements. Seismic technology and GPR should be used together as damage should be expected when seismic tests indicate low modulus values in addition to anomalies shown using the GPR (7).

2.7 Moisture Susceptibility Testing

While testing methods for determining the moisture susceptibility of asphalt mixtures are far from perfect, tests have been developed which help characterize how well a mixture will perform from a moisture susceptibility perspective. In this section two popular tests, AASHTO T 283 and AASHTO T 324, and a less popular conditioning method will be discussed.

2.7.1 AASHTO T 283

The most common moisture susceptibility test currently conducted in the United States is AASHTO T 283 which results in a Tensile Strength Ratio. It has a long history of use by state DOTs and provides results which can be easily understood and specified for a pass or fail criteria. Simply put, the test provides a method to determine how well a mixture will perform after undergoing saturation, a freeze thaw cycle, and soaking in a hot water bath to represent environmental conditioning that will occur over the lifecycle of the pavement. The TSR is a widely used concept to determine if an asphalt mixture will be susceptible to moisture damage. Typically, the standard practice is to follow AASHTO T-283 “Resistance of Compacted Hot Mix Asphalt (HMA) to Moisture-Induced Damage.” This test consists of fabricating six samples to a height of 95±5 mm and 7±0.5% air voids. Three samples are conditioned by saturating between

70 to 80 percent of the voids before subjecting the samples to a freeze-thaw cycle. The remaining three samples are left as an unconditioned or control set. The samples are loaded diametrically in indirect tension until failure and the peak load values are recorded. The ratio between the average conditioned strengths (CS) and unconditioned strengths (UCS) is the TSR value ($TSR = \frac{CS}{UCS}$). According to AASHTO M323 the acceptable minimum requirement for laboratory compacted specimens is 0.80. Figure 2 below shows an illustration of the conditioning and loading procedure used for AASHTO T-283.

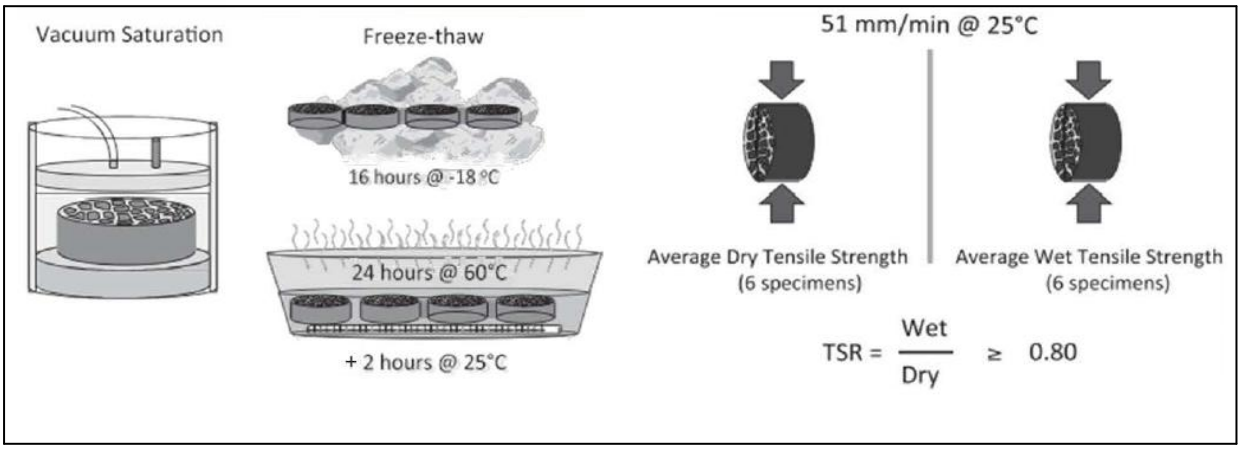

Figure 2. TSR Conditioning/Testing Procedure (15)

While AASHTO T283 is the most used test for determining moisture susceptibility in a mix, it has its shortcomings. As noted by Kringos et al. (16), there have been instances where mixes which performed well in the field had low tensile strength ratios (TSR), and vice versa. It is also noted that there are conflicting results on whether it is better to run the test with the 150-mm (6-in.) gyratory specimens or the 100-mm (4-in.) Marshall specimens as the former have results which are less variable and the latter have better correlation to field performance (16). There is also concern regarding the duration and severity of saturation with tests showing tensile

strength values from samples saturated at 55% significantly different from samples saturated at 80% (16). Other research indicated that in four case studies of stripping in asphalt concrete, the pavements were nearly 100% saturated which is significantly higher than the recommended levels of AASHTO T283 (17). Azari showed that the AASHTO T 283 specimens are exposed to large variations of the moisture conditioning of the samples, even when the moisture conditioning protocol is kept the same (18). He determined that the different compaction methods, Marshall vs. gyratory compaction, resulted in both different inside pore distribution and outside-porosity which affected the moisture accessibility of a sample (18). Additionally, Azari determined the vacuum saturation process must induce some micro-cracking inside the sample which contributes to the variability of the test (18). A final concern with AASHTO T 283 regards the nature of mechanical testing of the samples as some engineers have argued that a test which simulates the cyclic loading and pumping of traffic would be a more suitable test as opposed to loading samples with a constant rate (16).

2.7.2 Hamburg Wheel Tracking Device

The Hamburg wheel tracking device (HWTD) (AASHTO T 324) is a device used to analyze the susceptibility of asphalt mixes to moisture damage in a laboratory setting. It consists of a sample submerged in a water bath of 50°C typically but can range from 25 to 75°-C. The sample is loaded with a steel wheel applying a load of 705 ± 4.5 N (158 lb ± 1 lb). The wheel is repeatedly passed over the sample for 20,000 passes (10,000 cycles) or until a rut depth of 40.90 mm is reached. A maximum allowable rut depth of 4 mm at 20,000 passes is specified by the city of Hamburg, Germany (19), however, it has been suggested by the Colorado Department of Transportation that a less stringent criterion of 10 mm at 20,000 or 4mm at 10,000 passes be used (20). Samples can either be rectangular slabs compacted with a steel wheel or cylindrical

Superpave gyratory compactor (SGC) specimens. Izzo and Tahmoressi (21) determined the repeatability of the test results was not affected by the different compaction methods. Figure 3 below shows one setup for a Hamburg Wheel Tracking Device. Figure 4 shows a typical example of a passed sample (a.) and a failed sample (b.) using the SGC compaction method.

Figure 3. Hamburg Wheel-Tracking Device

a) Passed sample. b) Failed sample.

Figure 4. Typical Test Specimens with Different Rut Depths (22)

There are four main attributes of HWDT results (Figure 5). The first phase is considered the post compaction consolidation. The post compaction consolidation is the deformation in millimeters at 1000 wheel passes and occurs rapidly during the first few minutes of the test. This phase is referred to as the post-compaction consolidation because it is assumed that the rutting is actually the densification of the material under initial loading (22). The second stage is referred to as the creep slope and is considered to be related to rutting primarily from plastic flow (21). The stripping slope is the last portion of the data and relates primarily to the deformation due to moisture damage (21). The stripping inflection point (SIP) is the point where the creep slope intersects the stripping slope and is considered to be one of the most important parameters of the HWDT results as it is the point where permanent deformation primarily due to moisture damage is said to begin (22).

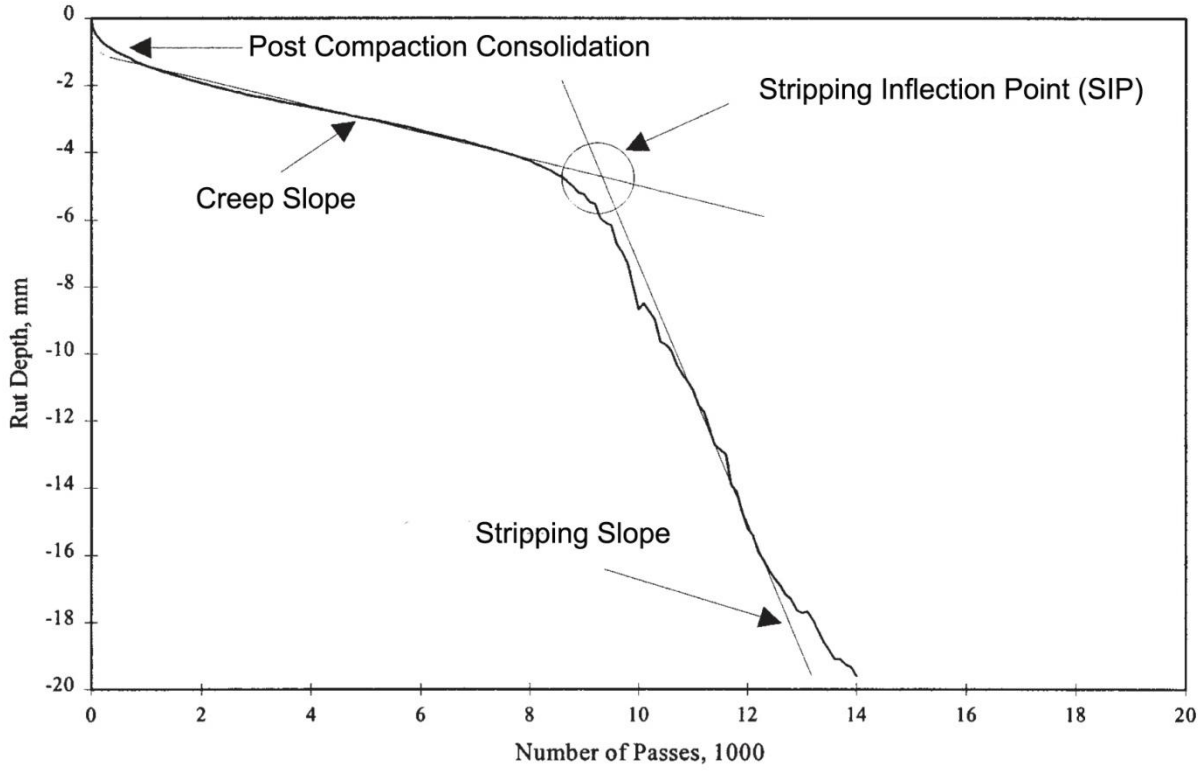

Figure 5. Test Results from HWDT (21)

Throughout the literature (19),(22)(23) the following conclusions have been made regarding the HWTD:

- This test has been shown to have the potential to discriminate between pavements with known field stripping performance and several levels of severity of moisture distress.
- There is excellent correlation between the stripping inflection point and the known stripping performance.
- Good pavements had stripping performances generally greater than 10,000 passes.
- Results show that HWTD is sensitive to aggregate properties that include clay content, high dust-to-asphalt ratios, and dust coating on the aggregates. This result suggests that aggregate quality is important to obtain passing results.
- Most of the asphalt binders failed in the HWTD with poorer aggregate. As a result, asphalt binders cannot be expected to overcome aggregate deficiencies.
- The testing temperature should be selected based on the high temperature environment the pavement will experience

2.7.3 Moisture Induced Stress Tester (MIST)

The MIST device is an alternative conditioning device which has been used to simulate moisture damage. While there is not much information regarding this machine, the MIST device is a machine developed by InstroTek to simulate the physical action of pavement pressure differential as traffic passes over the pavement. It consists of a pressurized environmental chamber which can be filled with water at the desired temperature in order to simulate the pressures induced by traffic loading. The MIST is a self contained unit that operates at 120 volts AC and includes a hydraulic pump and piston mechanism that is designed to cyclically add and relieve pressure inside the sample chamber. The testing procedure involves placing a 4 inch or 6 inch diameter sample of 1 to 6" thickness inside the sample chamber. The chamber is filled with

water and the lid is closed prior to starting the test. The machine will automatically heat the sample to 60°C and will start cycling between zero and 40 psi of pressure. The entire cyclic conditioning process takes approximately 3 hours, which allows asphalt practitioners to evaluate the mixture for susceptibility to moisture over time and to ensure that quality pavements have been constructed (24). Shrum evaluated the conditioned samples using indirect tensile methods and by determining the dynamic modulus (25). She determined that dynamic modulus is more sensitive to moisture damage than tensile strength ratio based on 1,000 conditioning cycles using MIST. Figure 6 shows this device with samples inside.

Figure 6. Moisture-Induced Stress Tester (MIST)

2.8 Warm Mix Asphalt (WMA) Moisture Susceptibility Concerns

With a steady increase in the use of warm mix technology it is important to evaluate the potential for moisture induced damage. Although specifications typically allow a small amount of residual moisture in the aggregate to be used when producing asphalt concrete, it has been

suggested that with the reduced temperatures needed for warm mix technology some aggregates may not dry to the specified criteria before being coated with asphalt in the mixing drum (26). Other possibilities for new moisture susceptibility stem from the variety of products used to decrease the mixing temperature of asphalt concrete which will be discussed below.

2.8.1 Moist Aggregate

As warm mix technology results in a reduction of mixing temperature, some engineers are concerned that incomplete drying of virgin aggregate will occur in the drum increasing a mixture's susceptibility for moisture induced damage. In evaluations, researchers have shown that dry indirect tensile strength (ITS) values of mixtures containing moist aggregate decreased compared with mixtures containing dry aggregates; however, the decrease was offset with the addition of hydrated lime (26). Bennert, et al. reported similar results when performing tests which combined the reduction of mixing (production) temperature and increased initial moisture contents of the aggregate blend prior to mixing (27). Bennert's results indicated increased moisture damage susceptibility of the asphalt mixtures as measured using the TSR and the Hamburg Wheel Tracking test (27). In addition, the results indicated that moisture damage potential was greater for aggregate blends with higher absorption properties (27).

2.8.2 Aggregate Source

There are conflicting results on whether or not the aggregate source plays a significant role in the moisture susceptibility of WMA. Punith et al. performed tests on several non-foaming WMA additive mixtures containing moist aggregates. The study used two aggregate moisture contents, two lime contents, and two aggregate sources (28). A total of 34 mixtures were designed resulting in 340 specimens tested (28). The results indicated that the aggregate source significantly affected the ITS and rutting resistance regardless of the WMA additive, ASA, or

moisture content of the aggregate (28). However, Xiao, et al. indicated that the aggregate source (schist and granite) did not show a remarkable effect on moisture susceptibility of the mixtures in their study (29). While these two experiments report conflicting results on the effect of aggregate source, it is important to note that in both studies only two aggregate sources were used. It is possible that in one study the aggregates possessed similar characteristics which varied from the aggregate source in the other study. While neither of these studies were performed to specifically assess the effects of aggregate source on moisture susceptibility, other research has shown that aggregates with higher absorption properties posses a greater potential for moisture damage (27). As these results were based on one mix, this may not be the absolute case.

2.8.3 Warm Mix Technology Testing Results

Researchers have performed several experiments to assess the effects of WMA additives on the moisture damage susceptibility of asphalt concrete (AC) mixtures. A synthesis of these experiments follows.

Xiao et al. evaluated two WMA additives (Asphamin and Sasobit) at two moisture percentages (0%, and ~0.5% by weight of dry aggregate), and three hydrated lime contents (0%, 1%, and 2% by weight of dry aggregate). This was done to evaluate the influence of WMA additives and moisture content of aggregate on the anti-stripping resistance of asphalt mixtures. The mixtures were comprised of three aggregate sources and were tested using conventional moisture susceptibility testing procedures. The compaction temperature of 115°C to 121°C was used in this study regardless of WMA and aggregate type. The results indicated there were no statistical differences in indirect tensile strength (ITS) (wet or dry) values between a control mix, Asphamin mix, and Sasobit mix(25). While the addition of WMA additives generally had no

influence on the TSR values, the addition of lime played a key role in improving the ITS and TSR values, regardless of the mixture with or without moisture (26).

Goh indicated that the tensile strengths of foamed mixes were lower than the control mix while the TSR values were higher (30). Additionally, some of the foamed mixes produced at higher temperatures (115-130°C) showed TSR values greater than 1.0 indicating that there is a strength gain during the conditioning process (30).

A study performed to assess the use of reclaimed asphalt pavement (RAP) and WMA indicated that out of seven WMA technologies, only two technologies, both foaming, failed to meet the AASHTO recommended TSR value of 0.80. It was, however, noted that results from the TSR and HWTD were conflicting. Several mixtures which passed one test's failure criteria would fail the other test and vice versa. It was recommended that additional research be performed in order to determine the most appropriate method for evaluating the moisture susceptibility of WMA (31).

Advera, Sasobit, and Evotherm WMA additives were used in an experimental project on I-70 west of Denver Colorado. Results from the Colorado Department of using a modified Lottman procedure, similar to AASHTO T283, showed that while the Advera and Evotherm mixes performed worse than the HMA control mix, they still met the requirements, 80% for lab-produced samples and 70% for field-produced samples. Additionally, the Sasobit technology showed an increase in strength after the conditioning as indicated by a TSR value of 1.11 (32). This increase can be attributed to the properties of the Sasobit technology in that it is a form of wax which can cause an increase in stiffness to the binder.

When tests were performed using the HWTD, researchers found that none of the samples from the HMA control or the WMA test sections met the specification requiring less than 4 mm of rutting at 10,000 cycles. It was noted that CDOT does not typically test mixes on the HWTD that were designed to less than 100 gyrations which includes the mixes on this project at 75 gyrations. Visual observations indicated that the mixes failed primarily and initially due to plastic flow, not moisture susceptibility(32). It was suggested that this observation was an encouraging sign for the field performance related to moisture susceptibility. All mixtures had SIP values of 5,000 cycles or higher with the exception of the Advera mixture (32).

The conclusions for the CDOT experimental project using the modified Lottman test indicated that WMA may be more prone to moisture damage than the HMA control; however, all specimens met or exceeded the failure criteria. It was noted that after three years of evaluating, all test sections were in excellent condition regarding rutting, cracking, and raveling, and cores did not reveal any signs of moisture damage (32).

Evotherm has recognized the concern for moisture susceptibility in WMA and has included antistripping components in their chemical package (33). Hill performed a study to evaluate the effects of three WMA additives and production temperatures on asphalt mixtures. The three additives were Sasobit, Advera, and Evotherm M1. The production temperatures were 150, 125, and 100°C. One goal of the study was to evaluate the tensile strength ratios of WMA and HMA mixtures with varying air voids and WMA additives. Results indicated the use of Evotherm reduced the moisture sensitivity of the mix by consistently increasing the TSR values over the control values at all three mixing temperatures. However, it was noted that for this particular control mixture, common practice included a liquid anti-strip agent which was not used, and therefore the low TSR values for the control were not unexpected. The Sasobit mixture

showed results similar to the Evotherm mixture but to a lesser extent. Advera showed an increase in moisture sensitivity as temperatures decreased. While there was no clear evidence, it was stated that this was likely caused by the residual moisture present in Advera mixtures at lower production temperatures. In general, tensile strengths and TSR's dropped considerably with reductions in production temperature. Hill concluded each of the mixtures tested would likely need to include liquid anti-strip or hydrated lime to pass AASHTO T 283 and to better control stripping in the field as the values ranged from 45 to 66% excluding Evotherm which had no problems with TSR (34).

Based on these results, it appears that in general, moisture susceptibility of WMA mixes is similar to that of HMA mixes in terms of the failure criteria for TSR. These results suggest the continued need to evaluate moisture susceptibility on a mix by mix basis for WMA as current procedures suggest for HMA. The results of a survey on moisture damage in HMA pavements have been included in Appendix A. This survey was conducted by CDOT on August 4, 2002 (1).

Chapter 3: Materials

To assess the moisture susceptibility of asphalt mixtures, 87 mixtures were collected for laboratory assessment. Twenty six of the mixtures were collected in the summer of 2009 during reconstruction of the National Center for Asphalt Technology (NCAT) Test Track. Each Test Track mixture was collected at the Test Track and returned to the NCAT laboratories for further testing.

Figure 7. NCAT Test Track Materials Collection

The remaining mixtures from the National Cooperative Highway Research Program (NCHRP) project 9-47A were incorporated into these analyses to provide a more robust analysis. These mixtures were collected during construction for each of the NCHRP 9-47A projects.

The mixtures from both the Test Track and the NCHRP projects varied in terms of mixing and compaction temperatures, WMA technologies, RAP contents, asphalt binder grades, and binder modifiers. Table 1 provides basic information for the mixes sampled from the NCAT Test Track and

Table 2 provides some of the key mix properties from quality control testing obtained during construction.

Test Track conditions are unique in that the trafficking is designed to allow 10-15 years of truck damage to the pavement compressed into 2 years. Environmental conditions for the track are typical of southern Alabama which include high temperatures averaging in the upper 80s during summer months and mild winters averaging high temperatures in the upper 50s during winter months (°F).

Table 1. Basic Mix Information from Phase IV of the NCAT Test Track

Mix ID	Lift	Binder PG	Modifier	Gradation	Coarse RAP, %	Fine RAP, %	Hydrated Lime, %
N2	Surface	76 -22	SBS	PFC	15	0	0
N2	Base	67 -22	NA	Fine	0	0	0
S8	Base	67 -22	NA	Fine	0	0	0
S9	Surface	67 -22	SBS	Fine	0	0	0
S10	Surface	76 -22	WMA-Foam	Fine	0	0	0
S10	Intermediate	76 -22	WMA-Foam	Fine	0	0	0
S10	Base	67 -22	WMA-Foam	Fine	0	0	0
S11	Surface	76 -22	WMA-Additive	Fine	0	0	0
S11	Intermediate	76 -22	WMA-Additive	Fine	0	0	0
S11	Base	67 -22	WMA-Additive	Fine	0	0	0
N7	Surface	94 -xx	7.5% SBS	Fine	0	0	0
N7	Base	94 -xx	7.5% SBS	Fine	0	0	0
N5	Intermediate	67 -22	WMA-40% Thiopave	Fine	0	0	0
N5	Sub-Base	67 -23	WMA-30% Thiopave	Fine	0	0	0
N8	Surface	88 -22	7.5% SBS	Fine	0	0	0
N8	Intermediate	88 -22	7.5% SBS	Fine	0	0	0
S2	Surface	67 -22	NA	Coarse	0	0	1
S6	Surface	76 -22	SBS	Coarse	0	0	2
S7	Surface	76 -22	GTR	Coarse	0	0	2
N12	Surface	76 -22	SBS	SMA	0	0	1
N10	Surface	67 -22	NA	Fine	35	15	0
N10	Base	67 -22	NA	Fine	30	20	0
N11	Surface	67 -22	NA	Fine	35	15	0
N11	Base	67 -22	NA	Fine	30	20	0
S12	Surface	67 -28	TLA	Fine	0	0	0
S12	Base	67 -28	TLA	Fine	0	0	0

Table 2. Key Plant Mix Properties from QC Testing of Test Track Mixes

Mix ID	Lift	P_b %	P_{be} %	D/B	V_a %	VMA %	VFA %	Avg. Plant Temp. °F
N2	Surface	5.4	NA	NA	NA	NA	NA	335
N2	Base	4.7	4.3	1.9	3.0	13.0	77	315
S8	Base	4.9	4.4	1.2	3.6	14.0	75	325
S10	Surface	6.1	5.5	1.2	3.3	16.0	80	275
S10	Intermediate	4.7	4.1	1.3	4.6	14.3	68	275
S10	Base	4.7	4.2	1.2	4.1	14.0	71	275
S11	Surface	6.4	5.7	1.1	3.4	16.7	80	250
S11	Intermediate	4.6	4.0	1.2	4.9	14.5	66	250
S11	Base	5.0	1.5	1.2	3.0	13.7	78	250
N7	Surface	6.3	5.7	1.2	4.1	17.2	76	345
N7	Base	4.6	4.2	1.1	4.6	14.5	68	340
N5	Intermediate	5.7	5.3	0.9	4.5	17.1	74	275
N5	Sub-Base	6.2	5.8	0.8	2.3	16.1	85	275
N8	Surface	5.4	4.7	1.5	3.2	14.4	78	375
N8	Intermediate	4.4	3.8	1.2	4.9	14.0	65	340
S2	Surface	5.2	4.7	1.5	5.0	15.6	68	340
S6	Surface	5.4	4.5	1.2	4.5	14.8	70	345
S7	Surface	6.0	5.1	1.1	3.3	15.0	78	340
N12	Surface	6.3	6.3	1.7	4.0	18.5	78	340
N10	Surface	6.0	5.2	0.9	3.8	15.8	76	325
N10	Base	4.7	4.1	1.4	4.2	13.8	70	325
N11	Surface	6.1	5.3	0.9	3.2	15.5	79	275
N11	Base	4.6	4.0	1.3	4.1	13.7	70	275
S12	Surface	6.1	5.5	1.1	4.5	17.2	74	335
S12	Base	4.9	4.7	1.1	3.9	14.9	74	335

The mixes for the NCHRP 9-47A consisted of existing and new projects. This data are summarized below. While ideally the same mixture properties for all groups of mixes would be reported, due to limitations of available data from previous projects, this was not possible.

Traffic data for the "New Projects" ranged from an annual average daily traffic (AADT) count of 430 to as high as 59,000 with the majority of projects falling below 10,000. Traffic data for the existing projects was not available for this report. Environmental conditions for the 9-47A projects varied widely as the locations were spread throughout various states within the country.

Table 3. FHWA 9-47A "New Projects"

ST	Project	Technology	Recovered Binder True Grade	Anti-Strip	P_b	V_a	Compaction Temp. °F
	Walla Walla	HMA	77.9 -26.0	Superbond	5.66	3.4	300
WA	Walla Walla	Maxam Aquablack	75.3 -27.9	Superbond	5.11	3.4	250
	Centreville	HMA	88.3 -20.1	Pavebond Lite	4.99	4.2	310
VA	Centreville	Aztec DBG	89.5 -21.9	Pavebond Lite	5.4	2.75	260
	Escanba	HMA	59.0 -35.2	None	5.26	3.9	300
	Escanba	Advera	59.7 -35.2	None	5.34	3.4	250
MI	Escanba	Evotherm 3G	58.1 -34.8	None	5.0	3.0	250
	Baker	HMA	65.3 -31.2	Hydrated Lime	5.69	3.0	270
MT	Baker	Evotherm	65.2 -30.8	Hydrated Lime	5.76	4.0	235
	Griffith	HMA	74.6 -21.0	None	6.18	5.6	285
	Griffith	Gencor Foam	70.4 -22.8	None	5.61	5.6	240
	Griffith	Evotherm 3G	71.9 -23.2	None	5.95	6.4	230
IN	Griffith	Heritage Wax	72.5 -20.4	None	5.95	4.9	240
	Jefferson Co	HMA	92.5 -17.8	None	5.33	1.9	295
FL	Jefferson Co	Terex CMI Water Injection	90.4 -17.2	None	4.95	3.4	250
	Queens	HMA	74.6 -21.4	None	5.38	5.4	300
	Queens	BituTech Per	69.3 -24.9	None	5.48	5.6	225
	Queens	Cecabase	68.9 -26.2	None	5.66	3.0	225
NY	Queens	Sonnewarmix	70.1 -24.7	None	5.3	4.9	225

Table 4. Franklin, TN

Mix Type	Technology	Recovered PG	Antistrip %	P_b	V_a	Compaction Temp. °F
WMA	None	76.2 -22.5	0.3	5.2	2.73	N/A
WMA	Danley	74.3 -23.1	0.3	5.3	2.97	N/A
WMA	Advera	70.4 -24.3	0.3	5.2	3.1	230
WMA	Astec DBG	73.0 -23.7	0.3	5.0	2.9	230
WMA	Evotherm	72.9 -23.7	0.3	5.1	3.4	230
WMA	Sasobit	74.1 -22.1	0.3	5.1	3.9	230

Table 5. Silverthorne, CO

Mix Type	Technology	Recovered PG	Antistrip %	P_b	V_a	Compaction Temp. °F
HMA	None	59.9 -30.3	1	6.23	3.1	280
HMA	None	59.9 -30.3	0	6.41	3.0	280
HMA	None	59.9 -30.3	0	6.04	3.6	280
WMA	Advera	60.7 -30.4	1	6.38	1.8	250
WMA	Sasobit	64.2 -29.2	1	6.32	2.4	250
WMA	Evotherm DAT	N/A	1	6.38	2.2	250

Table 6. Royal, NE

Mix Type	Technology	Virgin PG	Recovered PG	P_b	V_a	Compaction Temp. °F
HMA	None	64 -28	74.5 -27.6	4.53	2.6	290
WMA	Evotherm	64 -28	68.6 -30.4	4.56	4.2	235
WMA	Advera	64 -28	69.7 -30.1	4.8	3.8	235

Table 7. Iron Mountain, MI

Mix	Technology	Virgin PG	P_b	V_a	Compaction

Type					Temp. °F
HMA	None	58 -34	5.42	4.1	300
WMA	Sasobit	58 -34	5.14	3.4	250

Table 8. Graham, TX

Mix Type	Technology	Recovered PG	P_b	V_a	Compaction Temp. °F
HMA	None	70 -16, 70 -22	4.86	N/A	290
WMA	Astec	70 -22	4.85	3.4	N/A

Table 9. Kimbolton, OH

Mix Type	Technology	RAP %	Virgin PG	P_b	V_a	Compaction Temp. °F
HMA	None	15	70 -22	5.48	1.8	300
WMA	Sasobit	15	70 -22	5.65	1.9	250
WMA	Evotherm	15	70 -22	5.68	1.15	250
WMA	Evotherm	15	70 -22	5.84	1.75	250
WMA	Zeolite	15	70 -22	5.5	2.05	250

Table 10. Macon, GA

Mix Type	Technology	RAP %	Recovered PG	P_b	V_a	Compaction Temp. °F
HMA	None	15	76.0 -21.7	5.69	1.9	235
WMA	Evotherm	15	74.9 -23.9	5.61	1.4	300
WMA	Rediset	15	75.4 -24.5	5.95	N/A	255
WMA	Ceca	15	77.9 -27.8	5.78	2.3	235

Table 11. Milwaukee, WI

Mix Type	Technology	RAP %	Virgin PG	P_b	V_a	Compaction Temp. °F
HMA	None	14	64 -28	5.07	3.7	300
WMA	Sasobit	14	64 -28	5.34	3.7	250
WMA	Evotherm	14	64 -28	4.98	2.9	250

Table 12. St. Louis, MO

Mix Type	Technology	RAP %	Virgin PG	Antistrip %	P_b	V_a	Compaction Temp. °F
HMA	None	10	70 -22	0.25	5.3	4.9	300
HMA	None	10	70 -22	0.25	5.3	4.2	250
WMA	Sasobit	10	70 -22	0.25	5.3	4.3	250
WMA	Sasobit	10	70 -22	0.25	5.3	3.7	250
WMA	Sasobit	10	70 -22	0.25	5.3	5.8	225
WMA	Sasobit	10	70 -22	0.25	5.3	4.1	225
WMA	Evotherm	10	70 -22	0.25	5.3	5.6	250
WMA	Evotherm	10	70 -22	0.25	5.3	5.2	250
WMA	Evotherm	10	70 -22	0.25	5.3	5.1	225
WMA	Evotherm	10	70 -22	0.25	5.3	4.1	200
WMA	Aspha min-Zeolite	10	70 -22	0.25	5.3	4.7	250

From Table 1 -

Table 12 it can be seen that there were a variety of mixtures to be tested. These mixtures came from various states and used several technologies. By having such a diverse selection of mixtures, the goal was to be able to obtain analyses which were robust and thus provide useful data regarding the technologies with respect to moisture damage performance. While Royal, NE, Kimbolton, OH, Macon, GA, and Milwaukee, WI were not part of the 9-47A projects, they were still included as part of the analyses.

The original goal of each project was to provide a control mixture to serve as the basis for comparison of different warm mix technologies. As the projects did not have this paper in mind during construction, the data was not collected in a manner for the direct comparisons presented later in this report. This explains why the data throughout the various 9-47A projects is not as in

depth and consistent as would be ideal for comparisons. Nonetheless, several of these projects provided additional data to incorporate into analyses such as HMA vs. WMA comparisons for various tests as well as hot field compaction versus lab reheated compaction results.

Chapter 4: AASHTO T 283 and Tensile Strength Ratio

4.1 Methodology of Testing

Each mix placed at the 2009 NCAT Test Track was evaluated for moisture susceptibility using the TSR methodology AASHTO T 283-07. The mixtures were reheated in the laboratory for approximately one hour until the mix was able to be transferred into a pan. Mixtures were heated to approximately 10-15 °F above the specified compaction temperature and compacted at a temperature specified to each mix. However, in addition to laboratory reheated specimens, TSR specimens for the surface mixtures which were part of the 2009 Group Experiment were compacted at the time of construction at the Test Track laboratory with mix which did not need to be reheated (35).

The mixes from Franklin Tennessee followed the ASTM D4867 method and did not include a freeze thaw cycle. Mixes from Colorado followed CDOT's modified Lottman method which is similar to AASHTO T 283. Mixes from Texas used a modified version of AASHTO T283 which followed the same saturation method but did not use a freeze thaw cycle. Due to the deviations in testing, these mixes were not included in the statistical analysis of the TSR results. Not all of the analyses included mixtures from each of the 9-47A projects as some data were not available on all of the projects. However, the remainder of the 9-47A projects were included as supporting data permitted.

Whether the mix was hot from the field or reheated in the lab, each sample was compacted using a Superpave gyratory compactor to a height of 95±5 mm and a diameter of 150 mm with air voids targeted between 6.5 and 7.5 percent. The AASHTO T283-07 procedure was followed. Figure 8 shows the device used to saturate the samples to the specified requirements. The indirect tensile strength including the unconditioned strengths (UCS) and conditioned strengths (CS) of each mixture was determined using a Pine Test Press (Figure 9). Figure 10 shows a sample with and without stripping post indirect tensile testing.

Figure 8. Saturation Apparatus

Figure 9. 850 Test Press by Pine Instrument Company

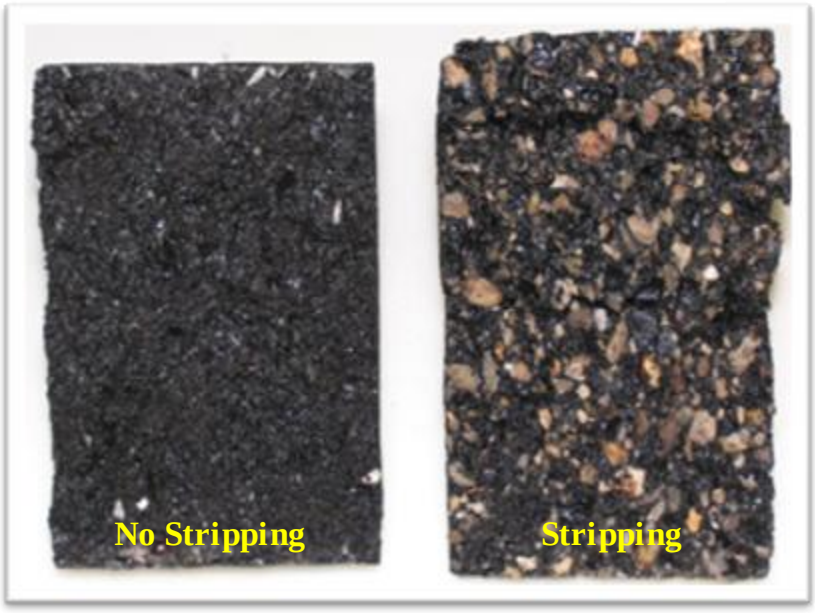

Figure 10. Typical TSR Specimen After Testing (Pavemeninteractive.org)

A typical data sheet showing results from an indirect tensile strength test is shown in Figure 11. Each curve represents one sample tested. The peak of each curve shows the maximum tensile strength that the particular specimen was able to withstand prior to failing.

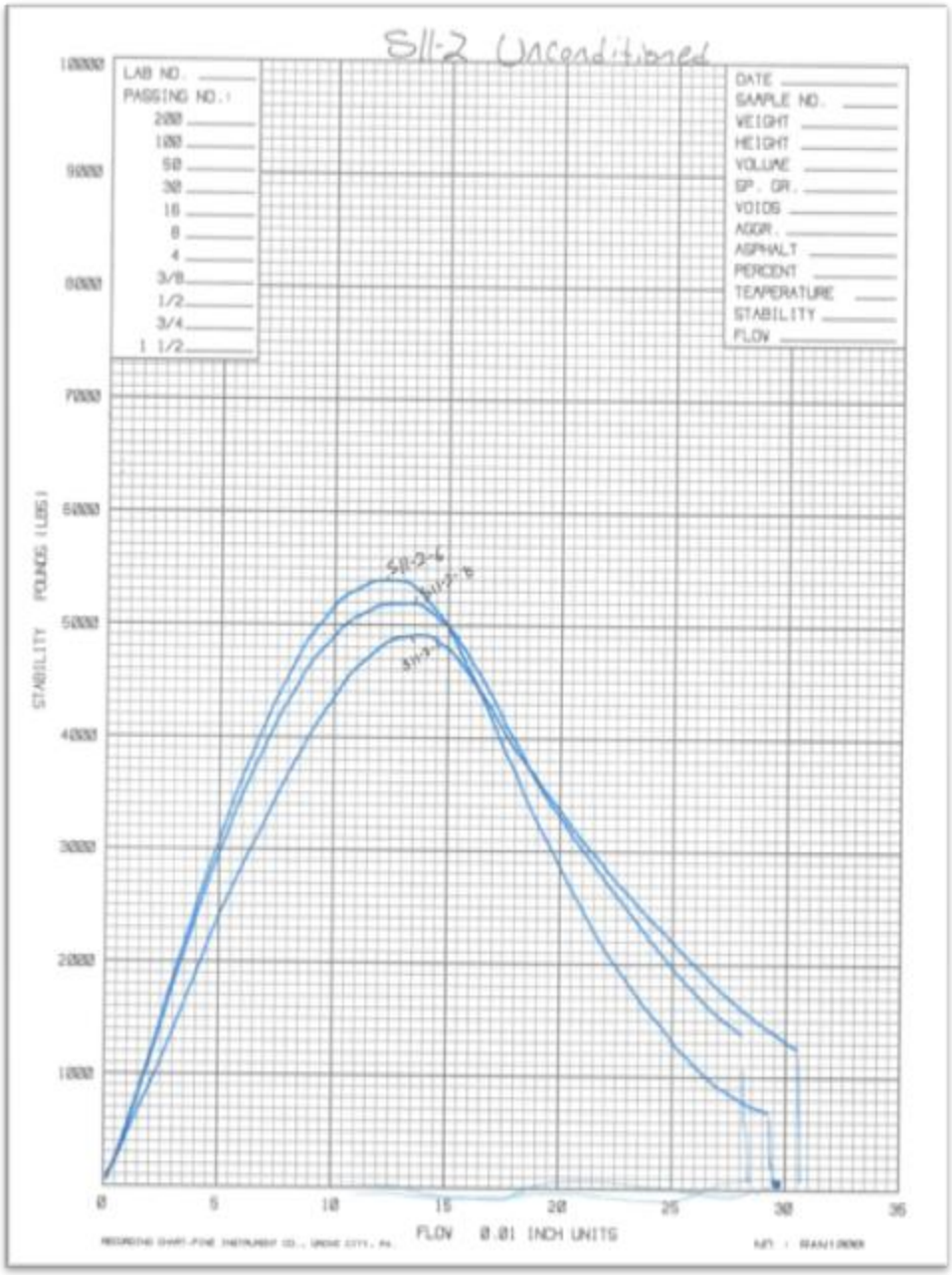

Figure 11. Indirect Tensile Strength Data

4.2 TSR Results

The results from the AASHTO T 283 testing are summarized in Table 13, Table 15, and Table 15. As can be seen very few mixtures failed the 0.80 minimum criteria for AASHTO M323. The mixtures which failed tended to be those with WMA technology. Further analyses and discussions regarding these results can be are displayed below. Once again it should be emphasized that not all projects are contained in each analysis due to data limitations.

Table 13. 2009 Test Track TSR Results

Mix ID	Layer	Mix Description	Compaction Temp., F	UCS Avg., Psi	CS Avg., Psi	Lab TSR
N2	Surface	Tacked FC-5	305	110.3	90.6	0.82
N2	Base	2006 N1-2	300	150.7	151.8	1.01
N5	Intermediate	Thiopave	250	156.4	103.3	0.66
N5	Sub Base	Thiopave	250	92.6	78.2	0.84
N7	Surface	Kraton	315	222.1	197.1	0.89
N7	Base	Kraton	315	237.6	208.4	0.88
N8	Surface	2006 N8-1	300	105.6	87.7	0.83
N8	Intermediate	2006 N8-2	300	139.4	164.9	0.85
N10	Surface	GE RAP	290	216.5	182.6	0.84
N10	Base	GE RAP	290	167.8	167.8	1.00
N11	Surface	GE RAP-WMA	245	198.9	161.3	0.81
N11	Base	GE RAP-WMA	245	192.3	153.3	0.80
N12	Surface	5:1 SMA	325	112.8	107.9	0.96
S2	Surface	RAP Surface	310	244.9	251.7	1.03
S6	Surface	SBS-Modified	315	171.4	148.1	0.86
S7	Surface	GTR-Modified	315	222.0	203.3	0.92
S8	Base	GE Control	290	134.6	116.2	0.86
S9	Surface	GE Control	310	145.4	137.2	0.94
S10	Surface	Foamed WMA	245	169.6	139.9	0.82
S10	Intermediate	Foamed WMA	245	153.0	129.4	0.85
S10	Base	Foamed WMA	245	132.7	108.0	0.81
S11	Surface	Additized WMA	220	125.0	106.4	0.85
S11	Intermediate	Additized WMA	220	149.6	135.6	0.91
S11	Base	Additized WMA	220	120.4	98.9	0.82
S12	Surface	GE+Special	295	176.3	145.2	0.82

S12	Base	GE+Special	295	165.4	173.6	1.05

Table 14. Test Track Hot-Compacted TSR Results

Mix ID	Layer	Mix Description	Compaction Temp., °F	UCS Avg., Psi	CS Avg., Psi	Field TSR
N10	Surface	GE RAP	290	187.2	162.5	0.87
N11	Surface	GE RAP-WMA	245	197.1	139.6	0.71
S9	Surface	GE Control	310	123.5	121.8	0.99
S10	Surface	Foamed WMA	245	128.4	87.7	0.68
S11	Surface	Additized WMA	220	130.7	106.9	0.82

Table 15. 9-47A "New Projects" TSR Results

State	Project	Technology	UCS Avg., Psi	CS Avg., Psi	Field TSR
MT	Baker	HMA	69.3	72.1	1.04
	Baker	Evotherm DAT	67.3	63.5	0.94
VA	Centreville	HMA	208.7	185.1	0.89
	Centreville	Aztec DBG	173.1	143.3	0.83
MI	Escanaba	HMA	52.4	50.0	0.95
	Escanaba	Advera	35.1	30.8	0.88
	Escanaba	Evotherm 3G	36.6	36.6	1.00
IN	Griffith	HMA	178.4	160.1	0.90
	Griffith	Gencor Foam	125.0	97.1	0.78
	Griffith	Evotherm 3G	132.7	110.6	0.83
	Griffith	Heritage Wax	158.7	131.3	0.83
FL	Jefferson Co.	HMA	217.3	198.1	0.91
	Jefferson Co.	Terex CMI Water Injection	208.7	159.6	0.76
NY	Queens	HMA	209.6	173.6	0.83
	Queens	BituTech PER	126.0	106.7	0.85
	Queens	Cecabase	144.7	121.7	0.84
	Queens	Sonnewarmix	143.3	114.9	0.80
WA	Walla Walla	HMA	135.1	119.7	0.89
	Walla Walla	Aquablack	118.8	101.9	0.86

4.3 Effect of Mixture Reheating on TSR Results

Engineers are commonly concerned with properly assessing the performance characteristics of asphalt mixtures. While under ideal conditions, performance test specimens

would be prepared directly after sampling the mixtures at the time of construction. In reality, it is difficult to prepare a large quantity and variety of performance test specimens to a narrow air void content tolerance in the field. To achieve specimens within the air void range for most performance tests, trial specimens must be first fabricated and tested to determine the proper sample weights correlating to the desired air voids for each specimen. Being able to perform these tasks simultaneously while preparing samples for quality control and quality assurance would require more time and resources than many contractors and departments of transportation are able to provide. Instead, quality control/quality assurance samples are typically compacted hot while additional mix is transported back to a laboratory where they are then reheated for mixture performance tests. This allows a more controlled setting in which the desired properties of the specimens can be obtained. However, this process has left many engineers wondering if reheating the mixture in the laboratory alters the performance properties of the asphalt mix.

Samples of plant-produced mix from five test track mixtures and 29 NCHRP 9-47A mixtures were used to determine how reheating mixtures in the laboratory would affect TSR results in comparison to compacting the mix hot in the field (See Table 16 below). As reheating may introduce an aging component to the results, these analyses were performed to determine if a significant difference was present. It is important to note that these specimens were fabricated from a split sample. The mixes were obtained from the truck and split into mix to be fabricated immediately and mix to be stored in buckets for later fabrication in the laboratory.

After completing the previously described TSR methodology, the TSR values for the hot-compacted and reheated mix samples were evaluated using a paired t-test analysis ($\alpha = 0.05$). The test results indicated there were no statistical difference (p-value = 0.703) between the TSR results of hot-compacted and reheated specimens. In some cases it was observed that there did

appear to be an effect; however, when taken as a whole, the data do not indicate a difference on TSR. UCS results indicated there was a significant difference (p-value = 0.00) between hot-compacted and reheated specimens. While the CS data (p-value = 0.052) does not meet the alpha of five percent, it is very close and may be considered significant from a practical standpoint. Because both the UCS and CS data are considered significantly different while the TSR data was not, it seems as though the reheating process does seem to have an effect on the physical properties of the mixture. Reheating seems to have a relatively equal effect on both the UCS and CS data such that when the ratio between the two results in a TSR the values are still similar. This indicates that TSR alone is not a sufficient indicator of moisture susceptibility and the other parameters, UCS and CS, should be looked at as well.

When the data were separated between HMA and WMA the paired t-test results were similar with no statistical difference between the two technologies (p-value = 0.94 and 0.71 respectively) regarding whether or not one technology is more susceptible to differences between hot compacted and reheated mixtures.

While there may be some variability due to the differences between hot-compacted and reheated specimens, Azari suggested that a comparison of strength values reported by different laboratories was not advisable due to lack of consistent calibration between laboratory equipment from one laboratory to another (18). He also determined the acceptable range of two TSR results when performed by a single operator was 9%, and as high as 25% when more than one laboratory was involved in obtaining testing results (18). As AASHTO T283-07 did not contain any precision and bias information, it was decided that comparisons made between hot-compacted specimens and reheated specimens would be evaluated under the precision statement that an allowable difference of 25% was considered typical between different laboratories.

While the saturation and indirect tensile strength testing for both hot-compacted and reheated specimens were all completed in the same laboratory, 2-3 different operators were charged with breaking the samples over the course of the projects. Furthermore, the actual fabrication of the specimens did not take place using the same compaction equipment or environmental conditions, and therefore it was decided that using the multi-laboratory precision statement would better correlate to the testing.

Additional statistical analyses were performed on 16 mixtures by using two sample t-tests to evaluate the differences between hot-compacted specimens versus reheated specimens with respect to CS and UCS values. These results can be seen in Table 17 and Table 18. Prior to running the two sample t-test, an F-test was performed to determine whether the variances between the indirect tensile strengths for each mixture were equal. If the p-value for F-test was above 0.50, the two sample t-test was run assuming equal variances; otherwise the t-test was run assuming unequal variances. This value was chosen because there were only three replicates for the test and thus only three values to perform each analysis on.

Table 16. TSR Reheated vs. Hot Comparison

Mix ID	Mix Description	Reheated TSR	Hot TSR	Difference	Exceeds Precision for Multi-Lab
S9-1	GE Control	0.94	0.99	0.05	No
S10-1	Foamed WMA	0.82	0.68	0.14	No
S11-1	Additized WMA	0.85	0.82	0.03	No
N10-1	GE RAP	0.84	0.87	0.03	No
N11-1	GE RAP-WMA	0.81	0.71	0.10	No
Macon, GA	HMA	0.92	0.87	0.05	No
Macon, GA	Evotherm 3G	0.92	0.82	0.10	No
Macon, GA	Redi-set	1.02	0.90	0.12	No
Macon, GA	Ceca	0.94	0.91	0.03	No
Milwaukee, WI	HMA	0.90	0.94	0.04	No
Milwaukee, WI	Evotherm ET	0.63	0.96	0.33	Yes
Milwaukee, WI	Sasobit	0.82	0.92	0.10	No
Royal, NE	Evotherm DAT	0.93	1.00	0.07	No
Royal, NE	Evotherm DAT	1.00	0.97	0.03	No
Royal, NE	Advera	0.99	1.00	0.01	No
Royal, NE	Advera	1.08	1.01	0.07	No
St. Louis, MO	HMA	0.97	0.76	0.21	No
St. Louis, MO	HMA	0.86	1.02	0.16	No
St. Louis, MO	Sasobit	0.85	0.69	0.16	No
St. Louis, MO	Sasobit	0.87	0.86	0.01	No
St. Louis, MO	Sasobit	0.84	0.68	0.16	No
St. Louis, MO	Sasobit	0.85	0.59	0.26	Yes
St. Louis, MO	Evotherm ET	0.81	0.95	0.14	No
St. Louis, MO	Evotherm ET	0.82	0.85	0.03	No
St. Louis, MO	Evotherm ET	0.81	0.67	0.14	No
St. Louis, MO	Evotherm ET	0.64	0.76	0.12	No
Kimbolton, OH	Evotherm ET	0.85	0.68	0.17	No
Kimbolton, OH	Evotherm ET	0.42	0.74	0.32	Yes
Kimbolton, OH	Evotherm ET	0.59	0.82	0.23	No
Kimbolton, OH	Evotherm ET	0.42	0.64	0.22	No
Kimbolton, OH	Sasobit	0.71	0.73	0.02	No
Kimbolton, OH	Sasobit	0.79	0.87	0.08	No
Kimbolton, OH	Aspha-min	0.55	0.71	0.16	No
Kimbolton, OH	Aspha-min	0.75	0.74	0.01	No

Table 17. CS Comparison Hot Compacted vs. Reheated

Mix ID	Technology	Hot or Reheated	F Test, p-value	Avg. CS	t-test, p-value
S9-1	GE Control	Hot	0.197	119.80	0.514
		RH		114.41	
S10-1	Foamed WMA	Hot	0.154	72.80	0.063
		RH		114.37	
S11-1	Additized WMA	Hot	0.000	94.20	0.089
		RH		111.10	
N10-1	GE RAP	Hot	0.882	132.90	0.378
		RH		124.99	
N11-1	GE RAP-WMA	Hot	0.306	124.70	0.569
		RH		119.68	
Macon, GA	Control	Hot	0.573	151.53	0.295
		RH		146.38	
	Evotherm 3G	Hot	0.206	124.04	0.185
		RH		118.08	
	Redi-set	Hot	0.684	102.55	0.218
		RH		113.40	
	Ceca	Hot	0.601	91.86	0.748
		RH		92.93	
Milwaukee, WI	Control	Hot	0.163	103.17	0.011
		RH		126.80	
	Evotherm ET	Hot	0.180	46.03	0.942
		RH		45.77	
	Sasobit	Hot	0.462	109.60	0.012
		RH		98.40	
Royal, NE	Evotherm DAT	Hot	0.351	88.35	0.074
		RH		106.07	
	Evotherm DAT	Hot	0.780	83.67	0.000
		RH		108.47	
	Advera	Hot	0.260	91.29	0.025
		RH		122.46	
	Advera	Hot	0.381	91.95	0.049
		RH		110.89	

Table 18. UCS Comparison Hot Compacted vs. Reheated

Mix ID	Technology	Hot or RH	F-test, p-value	Avg. UCS	t-test, p-value
S9-1	GE Control	Hot	0.146	99.03	0.230
		RH		120.60	
S10-1	Foamed WMA	Hot	0.550	117.00	0.039
		RH		140.13	
S11-1	Additized WMA	Hot	0.477	105.78	0.050
		RH		127.70	
N10-1	GE RAP	Hot	0.312	145.92	0.463
		RH		139.20	
N11-1	GE RAP-WMA	Hot	0.491	156.79	0.073
		RH		136.90	
Macon, GA	Control	Hot	0.293	173.40	0.072
		RH		159.39	
	Evotherm 3G	Hot	0.685	151.63	0.002
		RH		127.87	
	Redi-set	Hot	0.498	113.64	0.357
		RH		110.81	
	Ceca	Hot	0.601	100.87	0.688
		RH		99.20	
Milwaukee, WI	Control	Hot	0.609	109.57	0.000
		RH		140.17	
	Evotherm ET	Hot	0.000	47.90	0.008
		RH		72.13	
	Sasobit	Hot	0.423	118.70	0.761
		RH		120.23	
Royal, NE	Evotherm DAT	Hot	0.963	88.09	0.001
		RH		113.93	
	Evotherm DAT	Hot	0.506	86.31	0.003
		RH		108.14	
	Advera	Hot	0.450	91.65	0.001
		RH		123.09	
	Advera	Hot	0.444	91.25	0.072
		RH		102.81	

4.4 Effect of WMA Technology on Indirect Tension Strengths and TSR Results

As previously described in Chapter 2, one concern among many practitioners is WMA will negatively influence the moisture susceptibility of asphalt concrete. To assess this concern, a paired t test ($\alpha = 0.05$) was used to compare WMA mixtures to their HMA control mixture counterpart. When the results from both the laboratory and field compacted mixtures were combined and the data evaluated in a singular analysis, the paired t-test showed that WMA mixtures had statistically lower ($p = 0.001$) TSR values than HMA mixtures.

While the initial analysis showed there were statistical differences between the TSR values of HMA and WMA, the dataset included both plant produced field compacted, and laboratory reheated laboratory compacted mixtures, some of which were of the same mix design. Therefore, the dataset was subdivided into hot-compacted and reheated results. In this analysis, hot-compacted WMA mixtures also had statistically lower TSR values ($p = 0.006$) than hot-compacted HMA mixtures. From a statistical viewpoint there was difference found between the reheated values from HMA and WMA TSR ($p = 0.052$); however, the value implies a significant difference from a practical viewpoint. It should be noted that the average WMA TSR was 0.81 versus 0.87 for HMA, these statistical test may not have been sensitive enough to this type of data. As a result of the large difference in average TSR values between the two technologies, it is evident that TSR values for WMA specimens compacted in the lab were generally lower than those of HMA specimens.

Additionally, paired *t*-tests ($\alpha = 0.05$) were conducted on average unconditioned strength (UCS) and conditioned strength (CS) data from WMA mixtures and their respective HMA control mixtures to determine if WMA affects tensile strengths (Table 19). The results indicated WMA UCS values for both hot-compacted and reheated mix were significantly lower with an

average difference of approximately 25psi (p=0.000, 0.000). CS values for both field and lab compacted specimens were also significantly lower for WMA with an average difference of approximately 30psi (p= 0.000, 0.000).

Table 19. Indirect Tensile Strength Results

Lab or Field Compacted	CS or UCS	Observations	*p*-value	HMA (psi)	WMA (psi)
Lab	UCS	22	0.000	147.41	123.45
Lab	CS	22	0.000	127.1	99.01
Field	UCS	20	0.000	153.64	122.95
Field	CS	20	0.000	137.16	101.32

Table 20 and Table 21 show results from two sample t-tests for CS and UCS comparisons between HMA and WMA mixtures. The general trend for the majority of the mixtures shows that WMA values are significantly lower than their HMA counterparts. These tables show results on a mix by mix and project by project basis.

Table 20. CS Comparison HMA vs. WMA

Mix ID	Technology	HMA or WMA	F Test, p	Avg. CS	t-test, p
S9-1	GE Control	HMA	0.081	114.41	0.061
	GE RAP	WMA		72.8	
	GE Control	HMA	0.275	114.41	0.074
	Additized WMA	WMA		94.2	
Walla Walla, WA	Control	HMA	0.204	119.7	0.192
	Maxam Aquablack	WMA		101.9	
Centreville, VA	Control	HMA	0.987	185.13	0.003
	Astec DBG	WMA		143.3	
Escanaba, MI	Control	HMA	0.472	49.97	0.002
	Advera	WMA		30.77	
	Control	HMA	0.378	49.97	0.006
	Evotherm 3G	WMA		36.57	
Baker, MT	Control	HMA	0.509	72.13	0.006
	Evotherm DAT	WMA		63.47	
Griffith, IN	Control	HMA	0.306	160.13	0.006
	Gencor Foam	WMA		110.6	
	Control	HMA	0.495	160.13	0.000
	Evotherm 3G	WMA		97.13	
	Control	HMA	0.055	160.13	0.082
	Heritage Wax	WMA		131.3	
Jefferson Co, FL	Control	HMA	0.069	198.11	0.018
	Terex Foam	WMA		159.64	
Queens, NY	Control	HMA	0.765	173.57	0.000
	BituTech PER	WMA		106.73	
	Control	HMA	0.289	173.57	0.011
	Cecabase	WMA		121.67	
	Control	HMA	0.241	173.57	0.010
	SonneWarmix	WMA		114.93	
Macon, GA	Control	HMA	0.787	151.53	0.002
	Evotherm 3G	WMA		124.04	
	Control	HMA	0.435	151.53	0.002
	Redi-set	WMA		102.55	
	Control	HMA	0.878	151.53	0.000
	Cecabase	WMA		91.86	
Milwaukee, WI	Control	HMA	0.104	103.17	0.003
	Evotherm ET	WMA		46.03	

	Control	HMA	0.702	103.17	0.006
	Sasobit	WMA		109.6	
Iron Mountain, MI	Control	HMA	0.671	54.77	0.003
	Sasobit	WMA		70.57	

Table 21. UCS Comparison HMA vs. WMA

Mix ID	Technology	HMA or WMA	F Test, p	Avg. UCS	t-test, p
S9-1	GE Control	HMA	0.433	99.03	0.092
	GE RAP	WMA		117.00	
	GE Control	HMA	0.987	99.03	0.232
	Additized WMA	WMA		105.78	
Walla Walla, WA	Control	HMA	1.000	119.7	0.124
	Maxam Aquablack	WMA		101.9	
Centreville, VA	Control	HMA	0.967	208.7	0.000
	Astec DBG	WMA		173.1	
Escanaba, MI	Control	HMA	0.270	52.4	0.006
	Advera	WMA		35.1	
	Control	HMA	0.239	52.4	0.007
	Evotherm 3G	WMA		36.567	
Baker, MT	Control	HMA	0.327	69.27	0.594
	Evotherm DAT	WMA		67.3	
Griffith, IN	Control	HMA	NA	NA	NA
	Gencor Foam	WMA		NA	
	Control	HMA	0.647	178.4	0.000
	Evotherm 3G	WMA		125.03	
	Control	HMA	0.218	178.4	0.065
	Heritage Wax	WMA		158.67	
Jefferson Co, FL	Control	HMA	0.069	217.34	0.152
	Terex Foam	WMA		208.69	
Queens, NY	Control	HMA	0.304	209.63	0.003
	BituTech PER	WMA		125.97	
	Control	HMA	0.105	209.63	0.004
	Cecabase	WMA		144.73	
	Control	HMA	0.105	209.63	0.004
	SonneWarmix	WMA		143.33	
Macon, GA	Control	HMA	0.475	173.4	0.014
	Evotherm 3G	WMA		151.6	
	Control	HMA	0.241	173.4	0.004
	Redi-set	WMA		113.64	
	Control	HMA	0.993	173.4	0.000
	Cecabase	WMA		100.87	
Milwaukee, WI	Control	HMA	0.579	109.57	0.000
	Evotherm ET	WMA		47.9	

	Control	HMA	0.588	109.57	0.022
	Sasobit	WMA		118.7	
Iron Mountain, MI	Control	HMA	0.791	53.93	0.001
	Sasobit	WMA		73.6	

As the TSR value is simply a ratio of the conditioned tensile strengths to the unconditioned tensile strengths, it is important to evaluate the relationship between the UCS, CS, and TSR values. Figure 12. UCS vs. TSR graphically portrays the relationship between UCS and TSR while Figure 13 shows the trends between CS and TSR. Both figures suggest there is not a strong relationship between the strength and TSR values. From this evaluation it has been concluded that mixtures with higher tensile strengths may not necessarily obtain higher TSR values and vice versa. An example of each of these scenarios was seen with the results from Escanaba, MI, and the Jefferson County, FL mixtures. Mixtures in Escanaba, MI had UCS and CS values ranging from 30-53 psi yet the TSR values ranged from 0.88 to 1.0. The mixture from Jefferson County, FL showed a UCS of 208.7 psi and a CS of 159.6 psi resulting in a TSR value of 0.76. These examples show both extremes of the situation; one with low tensile strengths and high TSR values, and the other with high tensile strengths and a failing TSR value.

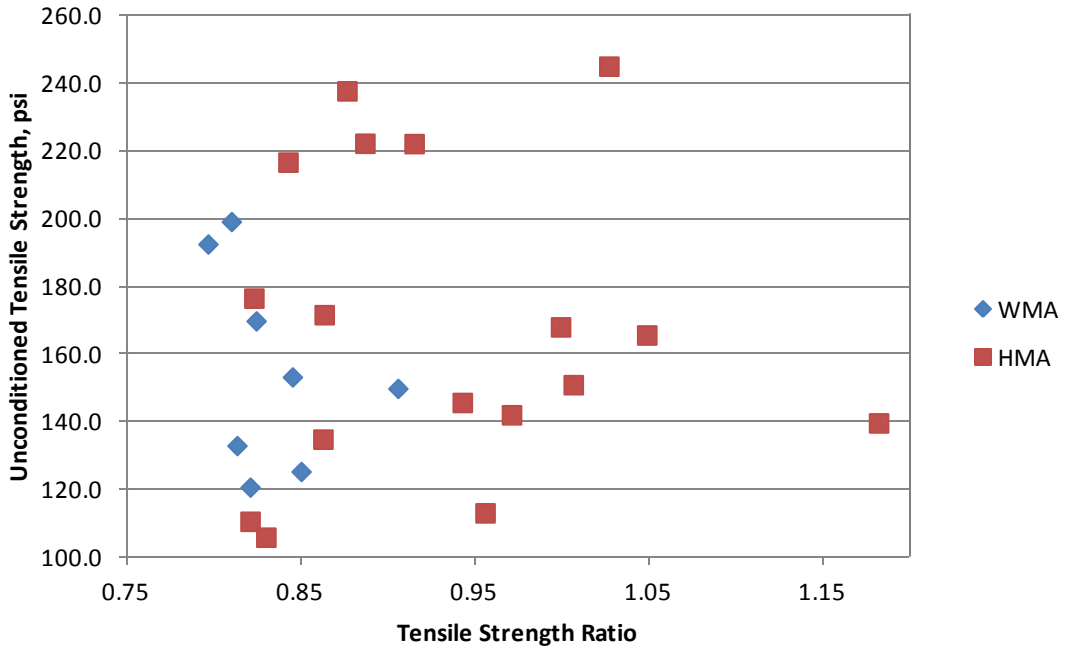

Figure 12. UCS vs. TSR

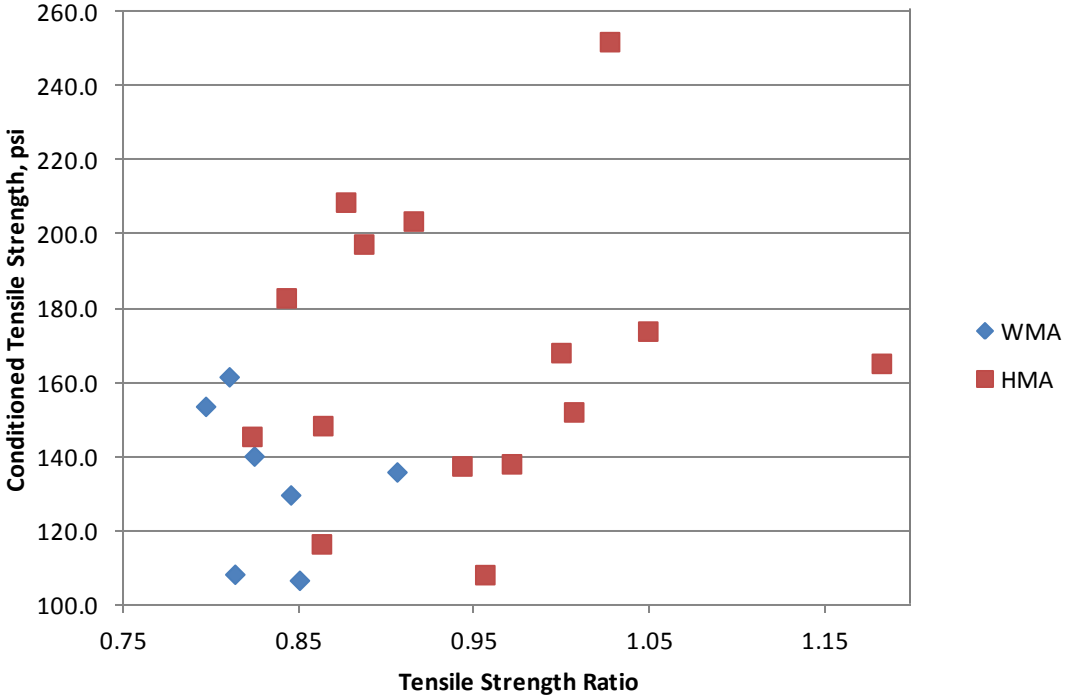

Figure 13. CS vs. TSR

In general, WMA mixtures tended to have statistically lower TSR values than their HMA counterparts. Additionally, both UCS and CS values for WMA were statistically lower than their HMA counterparts. These results may suggest the need for an anti-stripping additive in WMA mixtures to ensure that they will perform as well or better than HMA regarding moisture susceptibility. Because both the UCS and CS values were statistically lower, anti-strip agents may not increase the actual TSR value, but, they will help to increase the overall tensile strength of the mixture and provide better resistance to moisture damage.

Chapter 5: Hamburg Testing

In addition to AASHTO T 283, the Hamburg Wheel Tracking Device, AASHTO T 324, is a popular method to evaluate moisture susceptibility in asphalt concrete mixtures. While the device was originally developed to assess rutting susceptibility, it was later found that the test was useful in detecting moisture damage. The objectives of this chapter were to discuss the methodology of the HWTD and compare the results of HWTD testing between the mixtures tested in this study.

5.1 Methodology

The Hamburg Wheel-Tracking test was performed following AASHTO T324-07. Gyratory specimens from 23 Test Track mixtures and 47 NCHRP 9-47A mixtures were

compacted to 7±0.5% air voids and cut using a masonry saw to fit the Hamburg mold. After cutting, each sample was tested to ensure the specimens still met the previously stated air void criterion. The specimens were then placed in the mold and the water bath was filled. The temperature of the bath was allowed to reach a temperature of 50°C for 30 minutes prior to beginning the test. The test continued until 20,000 cycles were complete or until a linear variable differential transformer (LVDT) measured 20 mm of deformation, whichever came first. Three replicates were tested per mix.

The SIP value was determined from plotting the deflection versus the number of loading cycles and adding two trend lines, one for the creep slope and one for the stripping slope. The intersection of these two lines was selected as the SIP as illustrated in Figure 5. The particular HWTD used for this testing has been shown in Figure 14 below.

Figure 14. Hamburg Wheel-Tracking Device

The saw in Figure 15 was used to cut the samples to size to be place in the mold shown in Figure 16.

Figure 15. Masonry Saw

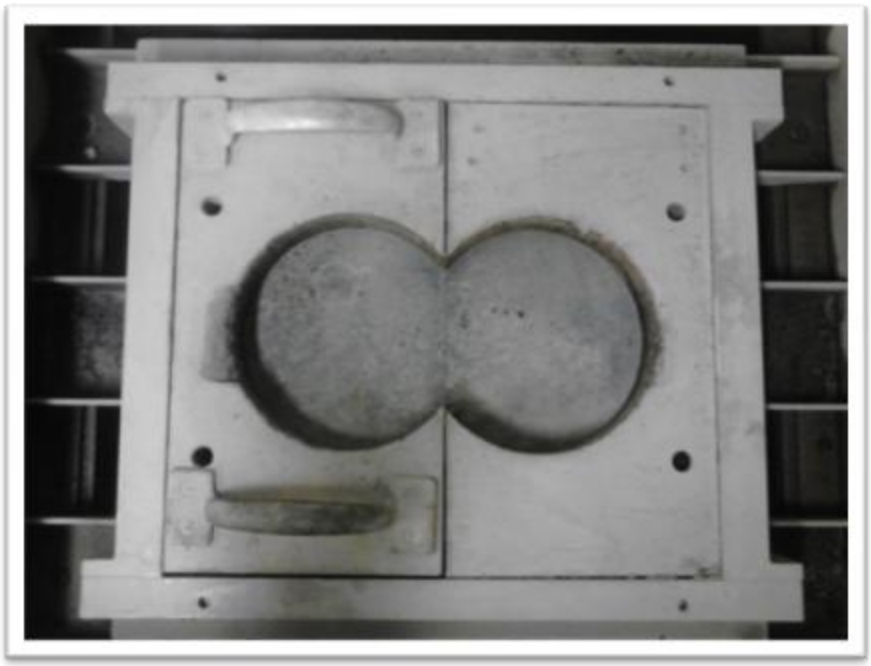

Figure 16. HWTD Mold

5.2 Hamburg Results

As expected, the results from the HWTD covered a wide range of SIP values. Given that the mixtures were from various parts of the country, the performance grade (PG) of the binder for each mixture may have had a significant impact on how each mixture performed. Because the test was run at 50° C, some mixtures may have been in a softer state than others and thus failed more rapidly. Even though mixtures from one part of the country performed differently than mixtures from other parts of the country, the analysis between a WMA mixture and its HMA control was evaluated to determine whether one technology performed better. Additionally, similar to the TSR analysis, hot-compacted vs. reheated mix specimen data were also analyzed from HWTD testing. Table 22 contains the SIP summary data from projects where AASHTO T324 testing was performed.

Table 22. SIP Summary Data

Project	Technology	Hot or Reheated	HMA SIP	WMA SIP
Baker, MT	Evotherm DAT	Hot	5,433	4,827
Centerville, VA	Astec DBG	Hot	10,000	10,000
Escanaba, MI	Advera	Hot	1,157	703
Escanaba, MI	Evotherm 3G	Hot	1,157	807
Graham, TX	Astec	Hot	7,250	6,575
Griffith, IN	Evotherm 3G	Hot	5,608	4,438
Griffith, IN	Gencor Ultrafoam	Hot	5,608	4,437
Griffith, IN	Heritage Wax	Hot	5,608	6,450
Jefferson, FL	Terex Foam	Hot	10,000	10,000
Kimbolton, OH	Sasobit	Reheated	10,000	7,950
Macon, GA	Evotherm 3G	Hot	5,200	6,100
Macon, GA	Redi-set	Hot	5,200	7,450
Macon, GA	Cecabase	Hot	5,200	3,950
Queens, NT	BituTech	Hot	9,202	3,722
Queens, NT	Cecabase	Hot	9,202	3,163

Queens, NT	Sonnearmix	Hot	9,202	3,798
Royal, NE	Evotherm DAT	Hot	4,170	3,850
Royal, NE	Advera	Hot	4,170	3,603
St. Louis, MO	Sasobit	Hot	7,850	8,550
St. Louis, MO	Evotherm ET	Hot	7,850	9,688
St. Louis, MO	Sasobit	Reheated	9,850	9,288
St. Louis, MO	Evotherm ET	Reheated	9,850	8,138
St. Louis, MO	Aspha-min	Reheated	9,850	10,000
Walla Walla, WA	Maxam Aquablack	Hot	5,767	8,167
9.5 mm 50% RAP	Astec DBG	Reheated	10,000	10,000
9.5 mm 50% RAP	Astec DBG	Hot	10,000	8,200
9.5 mm Control	Astec DBG	Hot	3,500	2,475
9.5 mm Control	Evotherm DAT	Hot	3,500	3,300
9.5 mm Control	Astec DBG	Reheated	6,200	5,550
9.5 mm Control	Evotherm DAT	Reheated	6,200	3,425

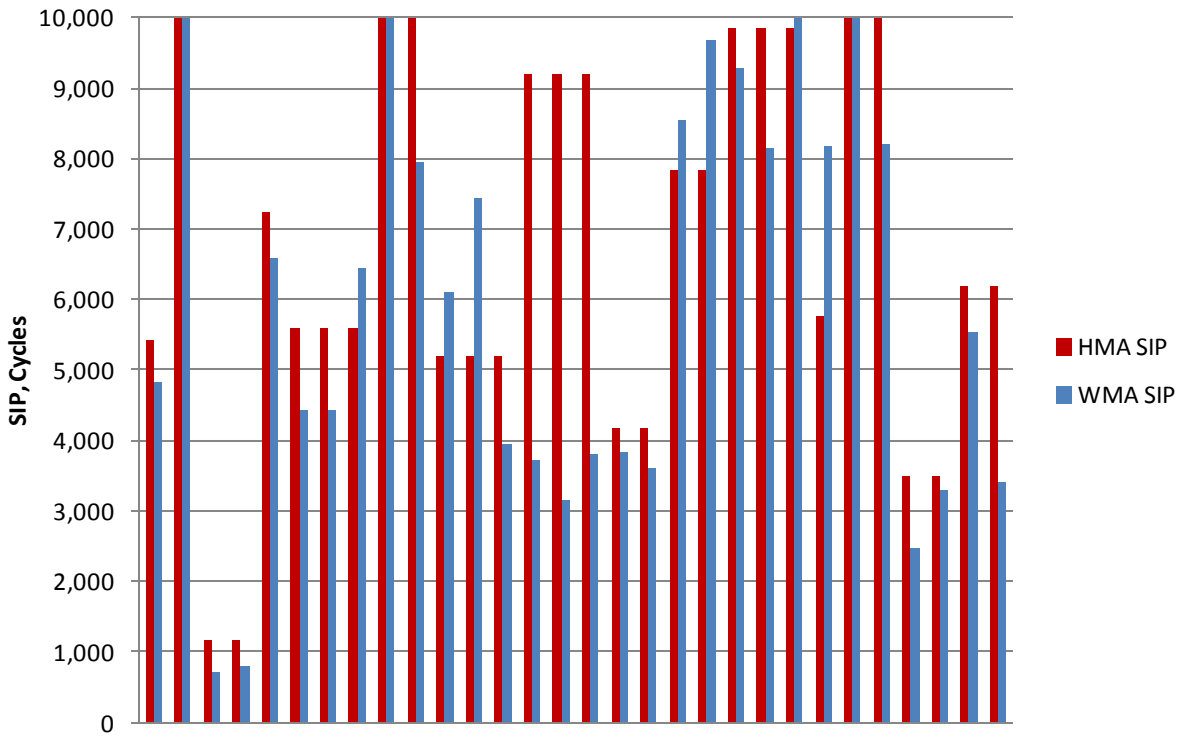

Figure 17. SIP HMA vs. WMA

5.3 Effect of Reheating on WMA Technology for Hamburg Results

As the same concerns with compacting in the lab versus compacting in the field for TSR are present in HWTD testing, a similar statistical analysis to that of the TSR results was used for analyzing the HWTD data. Again, the analysis used a paired t-test at a significance level of α=0.05 to evaluate whether there were differences in the results of the tests. To evaluate the SIP, five mixtures from the test track and 4 mixtures from NCHRP 9-47A were evaluated. With only eight degrees of freedom (DOF), the results indicated that there was not significant differences ($p = 0.052$) between the field and laboratory compacted specimens for the SIP, but again from a practical point of view the value is significant.

For the comparison between WMA and HMA, 30 mixtures (Table 22) in total were evaluated (six from the NCAT Test Track and 24 from NCHRP 9-47A). The results indicated that for the full dataset the WMA SIP values were significantly lower ($p = 0.029$) than their

HMA control counterparts. When the dataset was subdivided, the samples reheated and compacted in the laboratory showed lower SIP values for WMA ($p = .041$). Interestingly, the samples compacted in the field showed no differences between WMA and HMA in SIP values ($p = 0.113$).

The laboratory compacted samples seemed to follow the same trend as the TSR samples in that WMA displayed lower moisture damage resistance than the HMA control mixtures. The field data results indicated there was no statistical difference in SIP between the two technologies. This result may have been in part because a higher number of observations were used for the field compacted analysis and therefore it would represent a greater sample of the population.

Finally, a two sample t-test was performed on the 9-47A "New Projects" to evaluate the differences between HMA mixtures and their WMA counterparts. An F-test was first performed and if the resulting p-value was above 0.50 then the t-test assumed equal variances, if the p-value was below 0.50, the t-test assumed unequal variances. The results can be seen in Table 23 below and indicate only 3 of the 10 WMA SIP values significantly lower than the HMA control.

Table 23. 9-47A Paired t-test HMA vs. WMA SIP Results

Mix ID	Technology	HMA or WMA	F-test, p-value	Avg. SIP	t-test, p value
Walla Walla, WA	Control	HMA	0.010	5767	0.035
	Maxam Aquablack	WMA		8167	
Centreville, VA	Control	HMA	NA	10000	NA
	Aztec DBG	WMA		10000	
Escanaba, MI	Control	HMA	0.188	1157	0.168
	Advera	WMA		703	
	Control	HMA	0.280	1157	0.252
	Evotherm 3G	WMA		807	
Baker, MT	Control	HMA	0.266	5433	0.457
	Evotherm DAT	WMA		4827	
Griffith, IN	Control	HMA	0.066	5608	0.340
	Evotherm 3G	WMA		4438	
	Control	HMA	0.263	5608	0.360
	Gencor Foam	WMA		4437	
	Control	HMA	0.745	5608	0.512
	Heritage Wax	WMA		6450	
Jefferson Co., FL	Control	HMA	NA	10000	NA
	Terex	WMA		10000	
Queens, NY	Control	HMA	0.069	9202	0.011
	BituTech PER	WMA		3722	
	Control	HMA	0.161	9202	0.010
	Cecabase	WMA		3163	
	Control	HMA	0.466	9202	0.004
	SonneWarmix	WMA		3798	

5.4 Summary

Analyses showed that for SIP values, WMA had statistically lower results except when the analysis included only data collected from the field. The *p*-values shown in Table 24 which are lower than 0.05 indicate WMA results statistically lower than the HMA control counterparts. While the WMA values for SIP were expected to be lower, it is interesting that the field data indicated less of this trend. It is possible that an aging effect on the laboratory reheated samples could play a role in the quicker deterioration of the specimens.

Table 24. HWTD SIP *t*-test HMA vs. WMA

Dataset Type	*p*-value
Full	0.029
RH	0.041
Hot	0.113

Chapter 6 SIP Versus TSR

As the two most popular tests for predicting moisture induced damage in asphalt pavements are AASHTO T 283 and AASHTO T324, and it is of interest to assess how well the results from the two tests correlate to one another. Because the samples for both tests were split from the same mix, a direct comparison between the two tests can yield some practical results. A Pearson's correlation was performed to evaluate the relationship. The correlation values are dimension-free and fall between -1 and +1 (36). The extremes of this range correspond to the situations where all the points in a scatter plot fall exactly on a straight line with negative and positive slopes, respectively, and a correlation of zero corresponding to a situation where there is no linear association (36). The correlations between several variables of the two tests can be seen in Table 25 below where CS and UCS are the conditioned and unconditioned strengths of the TSR values, respectively.

Table 25. Pearson's Correlation Factors

Property	*Average SIP*	*CS (psi)*	*UCS (psi)*	*TSR*
Average SIP	1.0			
CS (psi)	0.7307	1.0		
UCS (psi)	0.7340	0.9612	1.0	
TSR	-0.0546	0.0294	-0.2351	1.0

From the table, the conditioned and unconditioned strengths correlate relatively well with the average SIP results indicating that a mixture with a higher tensile strength will likely have a correspondingly higher SIP. A less dominant trend can be seen between the average rut depth and the UCS, where the correlation is -0.62 indicating that as a mixture's tensile strength increases the rut depth for that mix will similarly decrease. This relationship seems to have a

solid foundation in basic engineering principles. The TSR and SIP values may be regarded as the most significant values for assessing the moisture susceptibility of an asphalt concrete mixture and thus the correlation between the two is important. Interestingly, this relationship had the second worst correlation between all of the variables analyzed at a value of -0.05. While this does not say that either of the tests is bad or that one is better than the other, it does indicate that the two tests do not fully agree on the moisture susceptibility of a mixture.

Figure 18 shows the TSR values versus the SIP values. Once again it can be seen that the two failure criteria do not fully agree. Setting the failure criteria for the SIP at 5000 passes resulted in 30.6% of the mixtures used passing the TSR requirement but fail the HWTD requirement. Additionally, only 59.2% of the mixtures passed both the criteria for moisture susceptibility. While these tests are used to evaluate whether or not a mixture will be susceptible to moisture damage in the field, the actual projects are not experiencing moisture damage which raises the question of whether the failure criteria for the tests is an accurate representation for field performance.

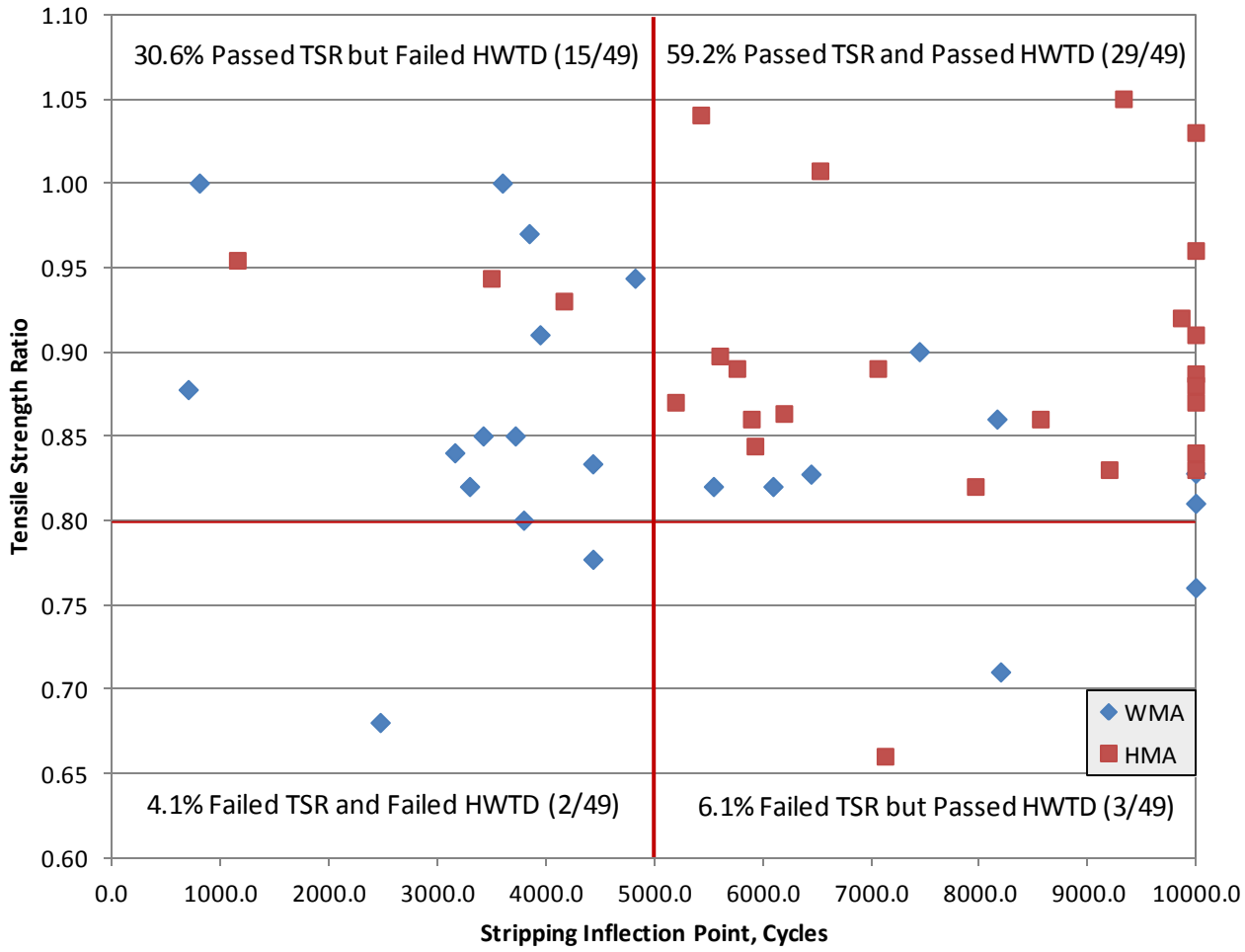

Figure 18. TSR and HWTD Failure Criteria

To further analyze how the data from the two tests related to one another the CS and UCS were plotted against the SIP values for each corresponding mixture. The plots displayed in Figure 19Figure 19. CS vs. SIP with SIP Ceiling and

Figure 21 show a positive correlation between the tensile strengths and SIP values of each mixture (R^2 = 0.66 and 0.64 for CS and UCS, respectively). There was concern that the data were skewed due to the artificial ceiling created by the SIP cutoff value of 10,000 cycles. To address this concern Figure 20 and Figure 22 were created by eliminating the data points at the 10,000 SIP value. Despite the concern, the trend was only strengthened slightly by the removal of the artificial ceiling (R^2 = 0.68 and 0.65 for CS and UCS, respectively).

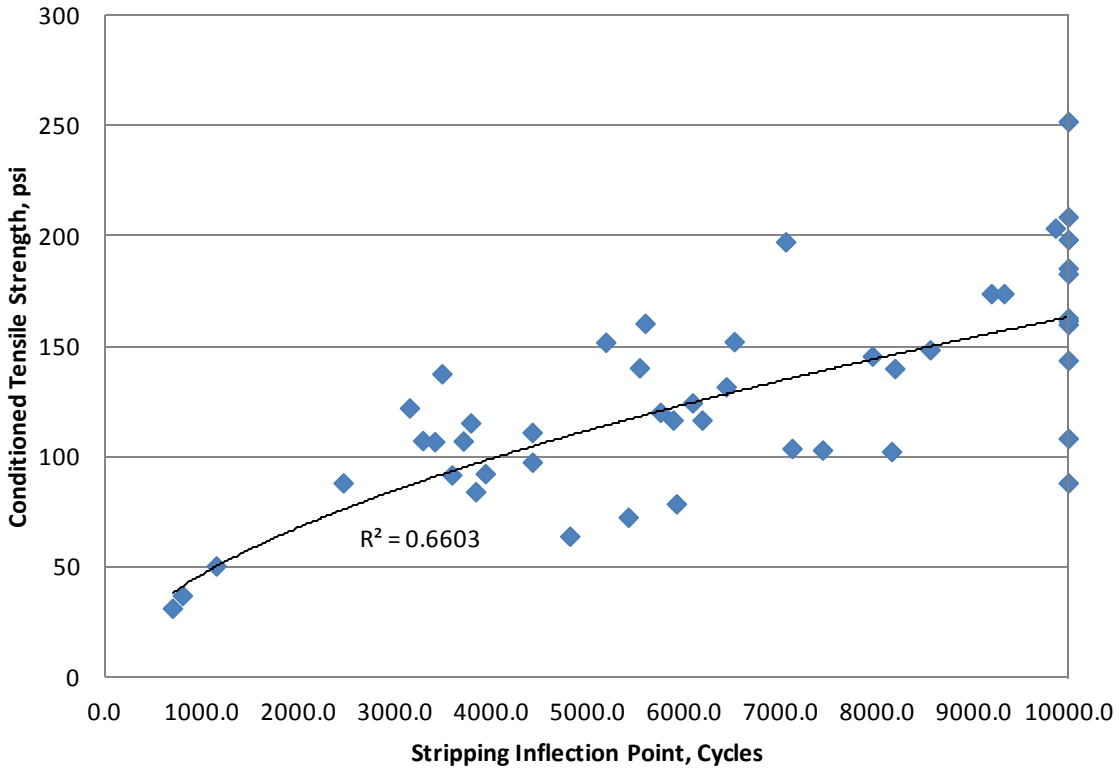

Figure 19. CS vs. SIP with SIP Ceiling

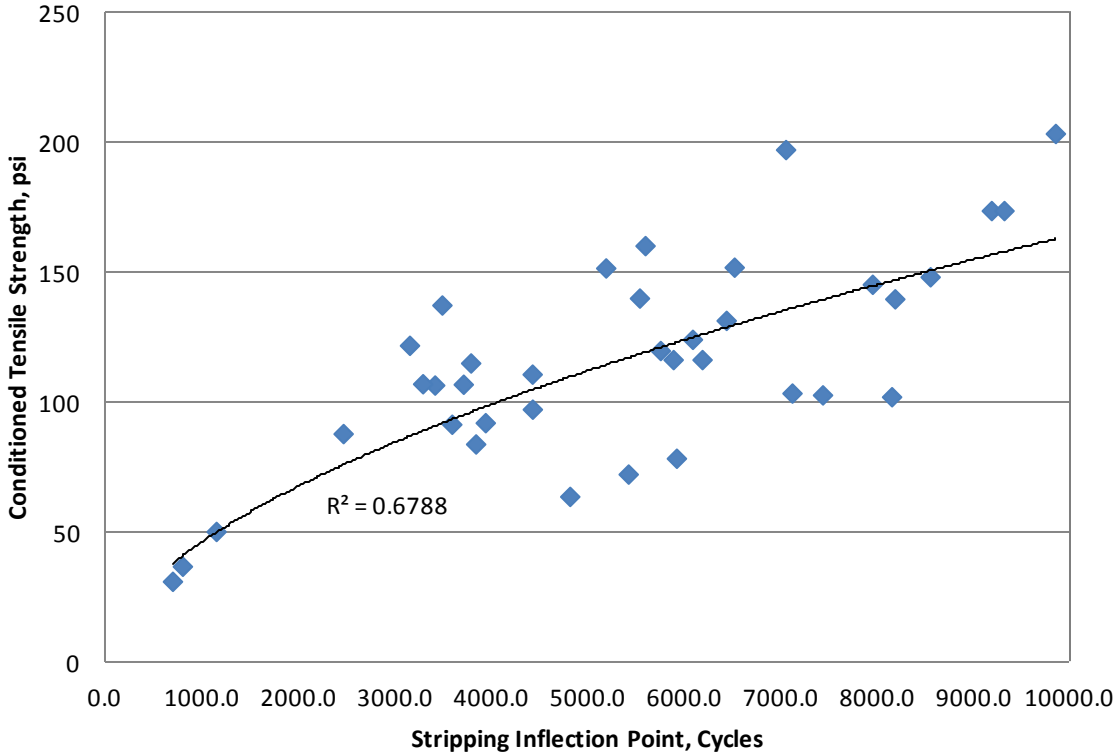

Figure 20. CS vs. SIP without SIP Ceiling

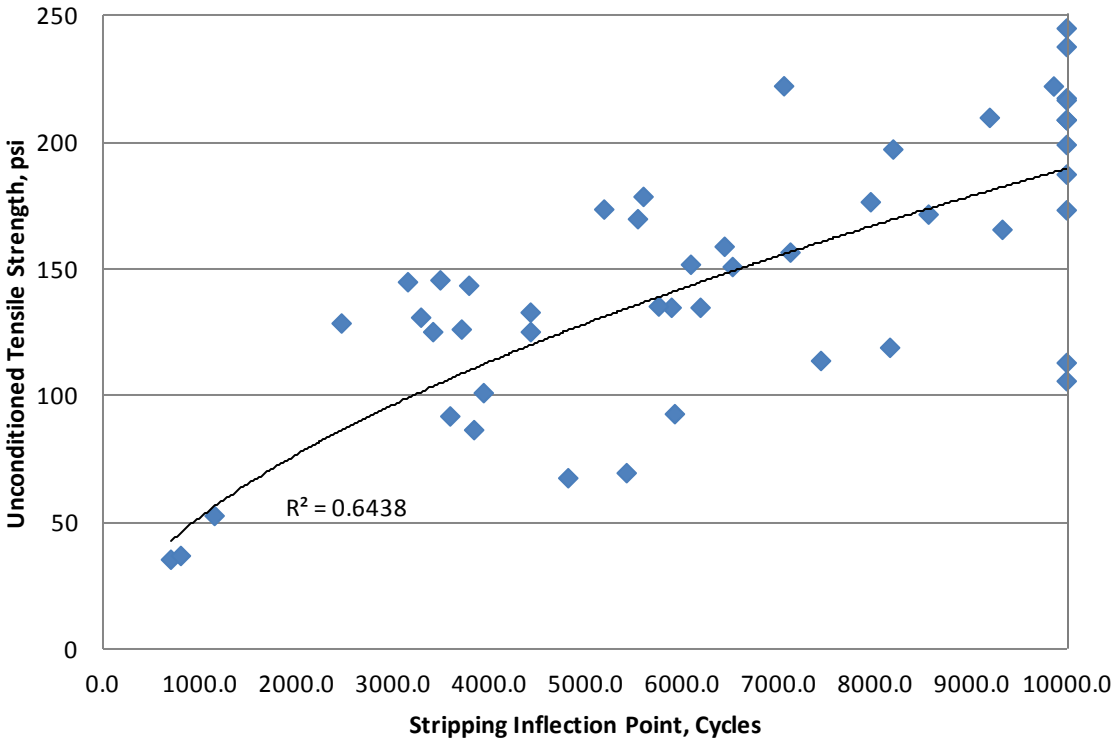

Figure 21. UCS vs. SIP with SIP Ceiling

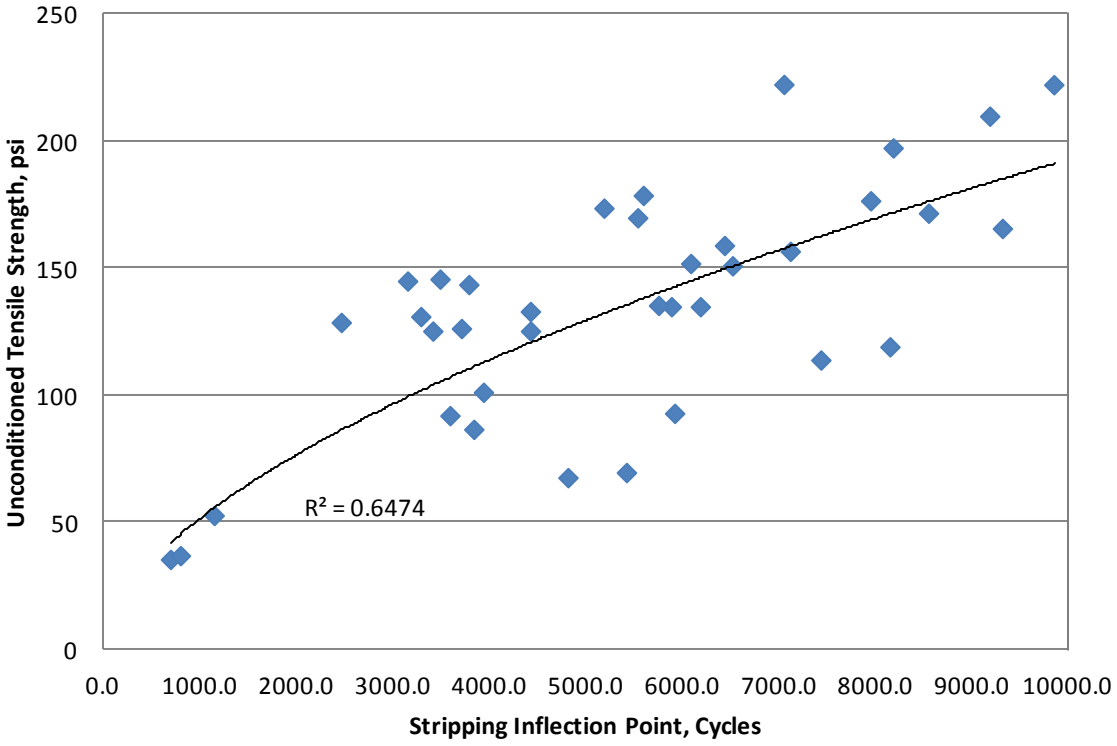

Figure 22. UCS vs. SIP without SIP Ceiling

6.1 Summary

The Pearson's Correlation indicated a relatively strong relationship between the average SIP and the CS and UCS values. The SIP and TSR values did not correlate well with one another. Figure 18 has graphically showed the lack of correlation between the two parameters.

By evaluating the mixtures which failed the 5000 cycle SIP criterion but were performing well in the field, it was discovered that 14 of the 17 mixtures were WMA while only three of the failing mixtures were HMA. This result indicated that a new testing temperature or SIP criteria may be needed in order to accurately analyze WMA HWTD results.

Chapter 7 Statistical Analysis of Critical HMA Properties Affecting Moisture Damage

As engineers seek to learn more accurate methods to test mixtures for moisture susceptibility, understanding how certain properties of a mix design affect the results of current practices may help to develop new testing protocols. To assess which mixture properties had the greatest influence on a mixture's susceptibility to moisture damage, several mixture properties were statistically analyzed to determine if a model could be developed to understand how mixture design would affect the UCS of a mix. These variables included the binder's recovered high binder grade (RHBG), volume of binder effective (Vbe), air voids (AV), and compaction temperature in °F (Temp). WMA technology was not included as a variable as it was not possible to quantify the different technologies. Instead, the compaction temperature served as the indicator between HMA and WMA.

7.1 UCS Model

The model was developed to assess which mixture properties best predicted the UCS results. As mixture data from the NCAT Test Track and 9-47A "New Projects" proved to be more comprehensive and consistent due to better data collection, it was determined that the model would be better developed using these data alone. With the data selected, Minitab® 16.1.0 was utilized to perform general regression analyses. The variables were all significant at a level of $\alpha \leq 0.05$. The final model for UCS included 34 observations and resulted in an R-squared value of 0.81.

$$UCS = -503.402 + 4.21384\ RHBG + 11.5473\ Vbe + 14.1336\ AV + 0.491349\ Temp \quad (1)$$

R-squared = 0.81

where: RHBG = recovered high binder grade

Vbe = volume of effective binder (%)

AV = air voids (%)

Temp = average plant temperature (°F)

While it is good that this model had a relatively high R squared value indicating it was able to estimate the indirect tensile strength of a mixture given the required information, the model itself should be used as a way of evaluating which mixture properties tend to have the most influence over the moisture related criteria. To determine which variables had the most influence on the model as a whole, the data were standardized. The standardization was performed because the model coefficients themselves do not accurately account for a variable's influence as the values for each variable can be vastly different in magnitude. The standardization process subtracts the mean value from the individual result and is then divided by the standard deviation. Equation 2 shows the approximate magnitude of influence each variable has on the model as a whole by the absolute value of the coefficients. The variables with a greater coefficient magnitude influence the model more than variables with lesser coefficient magnitudes.

$$UCS = 148.503 + 41.7183\ Z1 + 10.6818\ Z3 + 14.3758\ Z4 + 15.2422\ Z6 \quad (2)$$

R-squared = 0.81

where: Z_1 = RHBG

Z_2 = Vbe

Z_3 = AV

Z_4 = Temp.

It can be seen that the largest coefficient for the UCS model belongs to the recovered high temperature binder grade. This result follows that higher temperature binder grade will result in a stiffer mixture, and thus a higher tensile strength.

7.3 Summary

Mixture data from the 2009 Test Track and NCHRP 9-47A was used to develop a statistical model to estimate the values for UCS of an asphalt mixture and determine which mixture properties had the most influence on the final results. This model showed a relatively high R-squared value of 0.81 indicating that a high amount of variation in the data was explained by the resulting equations. Recovered high temperature binder grade was the dominant variable in the model.

Chapter 8 Lab to Field Comparison

The final objective of the research was to compare lab results to field performance. This was accomplished by evaluating texture results from the NCAT Test Track from the 2009 construction cycle (Figure 23).

Figure 23. NCAT Test Track

Pavement macrotexture refers to variations in the road surface in the range 0.02" (0.5 mm) to approximately 2" (50 mm) (37). The trafficking of the test section for the 2009 construction cycle was completed in early fall of 2011 and the texture results were obtained as a part of the final performance evaluation of the track. The texture data were collected using an Automatic Road Analyzer (ARAN) Inertial Profiler shown in Figure 24.

Figure 24. Automatic Road Analyzer (ARAN)

A comparison was made between the initial texture values obtained shortly after construction in 2009 and the final values obtained at the end of the research cycle in 2011. The idea for this evaluation stems from the possibility that sections which experienced large changes in texture over time indicate more raveling occurred, which may be related to moisture damage of the asphalt mixture. To assess possible relationships, both TSR and SIP values for each mixture were compared to the change in texture over 10 million Equivalent Single Axle Loads (ESALS) of trafficking. These results are shown in Figure 25 and Figure 26.

The lab results indicated there should not be problems associated with moisture damage for the mixtures from the Test Track. There was very weak correlation between texture change and TSR which was also the case between texture change and SIP. This may indicate that the texture changes observed on the track were not related to moisture sensitivity of the mixtures.

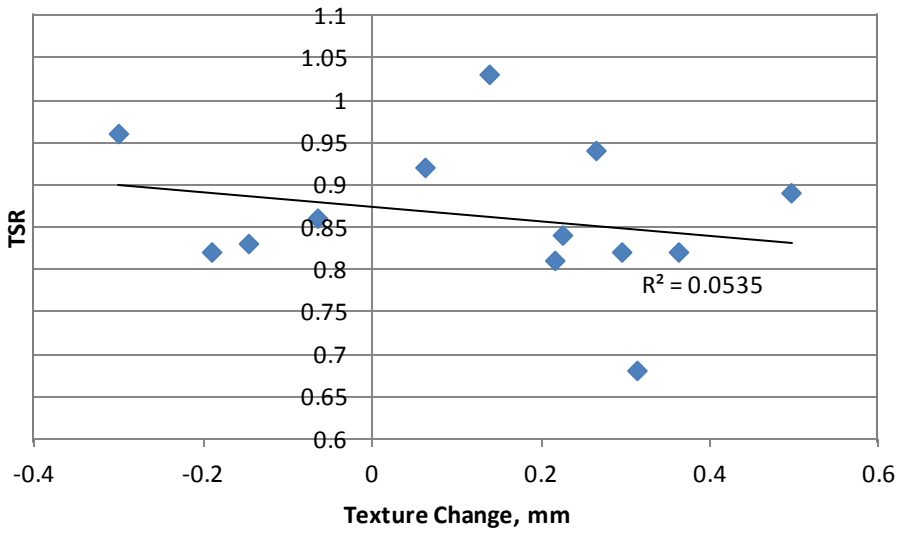

Figure 25. TSR vs. Texture Change, mm

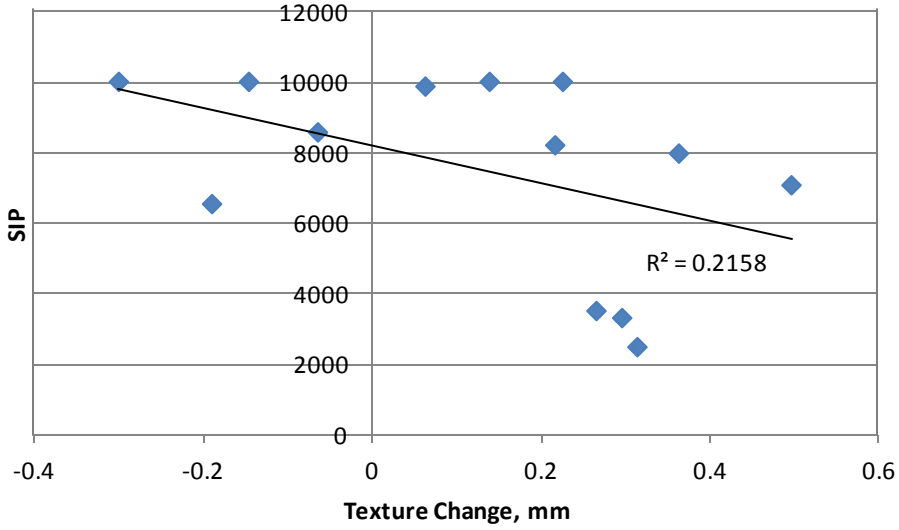

Figure 26. SIP vs. Texture Change, mm

Chapter 9 Conclusions and Recommendations

This study compared the moisture susceptibility of HMA and WMA based on the two most common moisture damage tests. Additionally, data were evaluated to determine whether a significant difference in test results could be attributed to fabrication of specimens in the field using fresh mix versus mix reheated in a laboratory. The following conclusions were drawn based on the results of this research:

- There was no significant difference ($\alpha = 0.05$, $p = 0.703$) between TSR samples compacted hot versus with specimens prepared from reheated plant mix.
- Given the practical statistical difference ($\alpha = 0.05$, $p = 0.052$) between HMA and WMA TSR values when compacted in the laboratory and average WMA TSR being 0.81 versus 0.87 for HMA, it is evident that WMA TSR values are significantly lower than their HMA counterpart mixtures.
- Results from the t-test which compared the combined laboratory and field mixture data indicated WMA had statistically lower TSR values ($\alpha = 0.05$, $p = 0.001$) than HMA.
- Both CS and UCS values were significantly lower for WMA mixtures than HMA mixtures regardless of whether they were compacted in the field or in the laboratory as p values were 0.000 ($\alpha = 0.05$).
- The tensile strength of a mixture is not an accurate indicator of its respective TSR value; however, the indirect tensile strength of the mixture does have a relative meaning to the mixture's performance.
- From a practical point of view, there was significant difference between hot versus reheated compacted specimens for SIP HWTD results ($\alpha = 0.05$, $p = 0.052$).

- In general WMA SIP values were significantly lower than their HMA counterparts ($p = 0.029$).
- The statistical model developed in this study showed a high correlation to the data provided with R square values at approximately 0.81 for the UCS model.
- Recovered high temperature binder grade was the dominant variable in predicting UCS.
- As no moisture related damage (raveling) occurred during the 2009 NCAT test track research cycle, surface texture data did not correlate to TSR or HWTD results.

The following recommendations are given based on the previously stated conclusions:

- A new SIP criteria or climate specific testing temperature is needed for testing WMA mixtures with the HWTD.
- It is recommended that testing temperature be more in tune with the environmental conditions for which the mix will be place as opposed to one specified testing temperature for all mixtures.
- Mix designers should continue to evaluate the need for anti-strip agents on a mix-by-mix basis regardless of whether or not HMA or WMA technology is used.
- Because the TSR value has shown a better correlation to actual field performance, AASHTO T 283 should be used for moisture susceptibility testing on WMA over AASHTO T 324 in its current state unless environmental factors are taken into account for testing.

References

(1) Hicks, R. G., Leahy, R. B., Cook, M., Moulthrop, J. S., Button, J., "Road Map for Mitigating National Moisture Sensitivity concerns in Hot-Mix Pavements." *Moisture Sensitivity of Asphalt Pavements: A National Seminar*, Transportation Research Board of the National Academies, Washington, D.C., 2003.

(2) Hicks, R. G. "Moisture Damage in Asphalt Concrete." *National Cooperative Highway research Program Synthesis of Highway Practice 175*, National Research Council, Washington, D.C., 1991.

(3) Asphalt Institute, "Cause and Prevention of Stripping in Asphalt Pavements." Educational Series No. 10 (ES-10), College Park, MD, 1981.

(4) Kiggundu, B. M., F. L. Roberts, "Stripping in HMA Mixtures: State-of-the-Art and Critical Review of Test Methods." *NCAT Report 88-2,* National Center for Asphalt Technology, Auburn University, September 1988.

(5) Tarrer, A. R., Wagh, V., "The Effect of the Physical and Chemical Characteristics of the Aggregate on Bonding." *Strategic Highway Research Program*, National Research Council, Washington, D.C., 1991.

(6) Majidzadra, K. and Brovold, F. N., "State of the Art: Effect of Water on Bitumen-Aggregate Mixtures." HRB, *Special Report 98,* 1968.

(7) Howson, J., Masad, E. A., Bhasin, A., Branco, V. C., Arambula, E., Lytton, R., Little, D., "System for The Evaluation of Moisture Damage Using Fundamental Material Properties." *Report No. FHWA/TX-07/0-4524-1*, Texas Transportation Institute, The Texas A&M University System, College Station, Texas, 2007.

(8) Hammons, M. I., Quintus, H. V., Geary, G. M., Wu, P. Y., Jared, D. M. "Detection of Stripping in Hot-Mix Asphalt." *Transportation Research Record 1949,* National Research Council, Washington, D.C., 2006, pp. 20-31.

(9) Kandahl, P. S., "Moisture Susceptibility of HMA Mixes: Identification of Problem and Recommended Solutions." *NCAT Report 92-1*, National Center for Asphalt Technology, Auburn University, May 1992.

(10) Anderson, D. A., Dukatz, E. L., and Petersen, J. C. "The Effect of Antistrip Additives on the Properties of Asphalt Cement." *Proceedings of the Association of Asphalt Paving Technologists (AAPT)*, Vol. 51, AAPT, Kansas City, Mo., 1982, pp. 298–317.

(11) Huang, B., Shu, X., Dong, Q., Shen, J. "Laboratory Evaluation of Moisture Susceptibility of Hot-Mix Asphalt Containing Cementitious Fillers." *Journal Of Materials in Civil Engineering*, Vol. 22, Issue 7, ASCE, New York, NY., 2010, pp. 667-673.

(12) Kim, Yong-Rak, Lutif, J. S., Bhasin, A., Little, D. N. "Evalutaion of Moisture Damage Mechanisms and Effects of Hydrated Lime in Asphalt Mixtures through Measurements of Mixture Component Properties and Performance Testing." *Journal Of Materials in Civil Engineering,* Vol. 20., Issue 10, American Society of Civil Engineers, New York, NY., 2008, pp. 659-667.

(13) Kennedy, T. W., Turnham, N. Jr., Epps, J. A., Smoot, C. W., Young, F. M., Button, J. W., Zeigler, C. D. "Evaluation of Methods for Field Applications of Lime to Asphalt Concrete Mixtures." *Proceedings of the Association of Asphalt Paving Technologists,* Vol. 52, AAPT, Kansas City, MO., 1983, pp. 508-534.

(14) Zaniewski, J., Viswanathan, A. G., "Investigation of Moisture Sensitivity of Hot Mix Asphalt Concrete." *Asphalt Technology Program*, Department of Civil and Environmental Engineering, Morgantown, WV, May 2006.

(15) Martin, A. E., Estakhri, C., "Moisture Sensitivity of WMA A Review & Look to the Future." *NCHRP 09-49*, Performance of WMA Stage I-Moisture Susceptibility, 2nd International Warm-Mix Conference, October 12th, 2011.

(16) Kringos, N., Azari, H., Scarpas, A., "Identification of Parameters Related to Moisture Conditioning That Cause Variability in Modified Lottman Test." *Transportation Research Record: Journal of the Transportation Research Board No. 2127,* Transportation Research Board of the National Academies, Washington, D.C., 2009 pp. 1-11.

(17) Kandhal, P., and I. Rickards, "Premature Failure of Asphalt Overlays from Stripping: Case Histories." *Asphalt Paving Technology,* Vol. 70, 2002, pp. 301-351.

(18) Azari, H., "Precision Estimates of AASHTO T283: Resistance of Compacted Hot Mix Asphalt (HMA) to Moisture-Induced Damage." *NCHRP Web-Only Document 166*, National Institute of Standards and Technology, Gaithersburg, MD, 2010.

(19) Aschenbrener, T., "Evaluation of Hamburg Wheel-Tracking Device to Predict Moisture Damage in Hot-Mix Asphalt." *Transportation Research Record No. 1492,* Transportation Research Board, National Research Council, Washington, D.C., 1995, pp. 193-201.

(20) Aschenbrener, T., R. L. Terrel, and R. A. Zamora., *"*Comparison of the Hamburg Wheel Tracking Device and the Environmental Conditioning System to Pavements of Known Stripping Performance*." Report CDOTDTD-R-94-1*, Colorado Department of Transportation, Denver, Colo., Jan. 1994.

(21) Izzo, R. P., Tahmoressi, M., "Use of the Hamburg Wheel-Tracking Device for Evaluating Moisture Susceptibility of Hot-Mix Asphalt." *Transportation Research Record 1681,* National Research Council, Washington, D.C., 1999, pp. 76-85.

(22) Yildirim, Y., Jayawickrama P. W., Hossain M. S., Alhabshi A., Cenk Yildirim, Smit A. F., Little, D., "Hamburg Wheel-Tracking Database Analysis." Texas Department of Transportation and Federal Highway Administration, FHWA/TX-05/0-1707-7, 2007.

(23) Stuart, K. D. and W. S. Mogawer, "Effect of Compaction Method on Rutting Susceptibility Measured by Wheel-Tracking Devices." Presented at the 76th Annual Meeting of the Transportation Research Board, Washington, D.C., January 12-16, 1997.

(24) "A Rational New Method of Moisture Sensitivity Testing." http://www.instrotek.com/pdfs/Article%20Asphalt%20Pro.pdf

(25) Shrum, E. D., "Evaluation of Moisture Damage in Warm Mix Asphalt Containing Recycled Asphalt Pavement." Master's Thesis, University of Tennessee, 2010.

(26) Xiao, F. Jordan, J., Amirkhanian, S. N., "Laboratory Investigation of Moisture Damage in Warm-Mix Asphalt Containing Moist Aggregate." *Transportation Research Record: Journal of the Transportation Research Board No. 2126,* Transportation Research Board of the National Academies, Washington, D.C., 2009, pp. 115-124.

(27) Bennert, T., Maher, A., Sauber, R., "Influence of Production Temperature and Aggregate Moisture Content on the Performance of Warm Mix Asphalt (WMA)." *Transportation Research Record: Journal of the Transportation Research Board No. 11-4037,* Transportation Research Board of the National Academies, Washington, D.C., 2011.

(28) Punith, V. S., Xiao, F., Amirkhanian, S. N., "Effects of Moist Aggregates on the Performance of Warm Mix Asphalt Mixtures Containing Non-Foaming Additives." *Journal of Testing and Evaluation*, Vol. 39, Issue 5, American Society for Testing and Materials, West Conshohocken, PA, 2011.

(29) Xiao, F., Zhao, W., Amirkhanian, F., "Laboratory Evaluation of Effects of Soaked Duration on Moisture Susceptibility of Warm Mix Asphalt Mix." *T&DI Congress 2011: Integrated Transportation and Development for a Better Tomorrow Proceedings of the first T&DI Congress 2011,* American Society of Civil Engineers, New York, NY., 2011.

(30) Goh, S. W. and You, Z., "Moisture Damage and Fatigue Cracking of Foamed Warm Mix Asphalt Using a Simple Laboratory Setup." *Journal of Materials in Civil Engineering*, American Society of Civil Engineers (ASCE), Reston, VA., 2011, pp. 1338-1345.

(31) Willis, R. J., West, R., Nelson, J., Taylor, A., Leatherman, K., "Combining Warm Mix Asphalt Technologies with Mixtures Containing Reclaimed Asphalt Pavement." 2nd International Warm-Mix Conference, October 12th, 2011.

(32) Aschenbrener, T., Schiebel, B., West, R., "Three-Year Evaluation of the Colorado Department of Transportation's Warm-Mix Asphalt Experimental Feature on I-70 in Silverthorne, Colorado: Final Report." *NCAT Report 11-02*, National Center for Asphalt Technology, Auburn University, May 2011.

(33) Prowell, B. D., Graham, C. H., Crews, E., "Field Performance of Warm-Mix Asphalt at National Center for Asphalt Technology Test Track." *Transportation Research Record: Journal of the Transportation Research Board No. 1998,* Transportation Research Board of the National Academies, Washington, D.C., 2007, pp. 96-102.

(34) Hill, B., Hakimzadeh, S., Buttlar, W. G., "An Investigation of the Effects of Three Warm Mix Asphalt Additives on Asphalt Binder and Mixture Properties." 2nd International Warm-Mix Conference, October 12th, 2011.

(35) West, R., Timm, D., Willis, R., Powell, B., Tran, T., Watson, D., Sakhaeifar, M., Brown, R., Robbins, M., Nordcbeck, A. V., Villacorta, F. L., Guo, X., Nelson, J., "Phase IV NCAT Pavement Test Track Findings." National Center for Asphalt Technology, Auburn University, February 2012.

(36) Ramsey, F. L., Schafer, D. W., "The Statistical Sleuth: A course in Methods of Data Analysis, Second Edition." *CENGAGE Learning,* Brook/Cole, Belmont, CA, 2002.

(37) Pulugurtha, S. S., Kusam, R. P., Patel, K., "Relationship Between Pavement Macrotexture and Crash Incidences on North Carolina Roads." *Final Report FHWA/NC/2007-12,* University of North Carolina at Charlotte, February 27, 2008.

Appendices

Appendix A

General Regression Analyses

General Regression Analysis: UCS

Regression Equation

UCS = -503.402 + 4.21384 RHBG + 11.5473 Vbe + 14.1336 AV + 0.491349 Temp

Summary of Model

S = 24.8399 R-Sq = 80.99% R-Sq(adj) = 78.36%
PRESS = 25726.6 R-Sq(pred) = 72.66%

Analysis of Variance

Source	DF	Seq SS	Adj SS	Adj MS	F	P
Regression	4	76213.2	76213.2	19053.3	30.8797	0.0000000
RHBG	1	63606.9	47749.3	47749.3	77.3871	0.0000000
Vbe	1	764.6	3292.5	3292.5	5.3361	0.0282026
AV	1	5359.3	6142.7	6142.7	9.9554	0.0037196
Temp	1	6482.3	6482.3	6482.3	10.5059	0.0029856
Error	29	17893.5	17893.5	617.0		
Total	33	94106.7				

Fits and Diagnostics for All Observations

Obs	UCS	Fit	SE Fit	Residual	St Resid	
1	150.70	135.398	8.8533	15.3023	0.65934	
2	134.60	153.410	7.2085	-18.8103	-0.79132	
3	128.40	170.545	10.1987	-42.1453	-1.86075	
4	153.00	173.661	9.2703	-20.6607	-0.89653	
5	132.70	122.551	7.3618	10.1489	0.42779	
6	125.03	159.440	13.4774	-34.4098	-1.64911	
7	149.60	147.186	11.2062	2.4144	0.10891	
8	120.40	95.952	9.3037	24.4480	1.06149	
9	244.90	235.971	10.1145	8.9286	0.39355	
10	171.40	171.432	9.6161	-0.0318	-0.00139	
11	222.00	189.671	9.3408	32.3285	1.40457	
12	216.52	218.537	9.5248	-2.0166	-0.08791	
13	167.80	226.816	10.2387	-59.0162	-2.60769	R
14	198.94	172.098	9.1979	26.8421	1.16330	
15	192.30	174.288	10.0339	18.0118	0.79267	
16	135.10	141.512	7.8920	-6.4115	-0.27222	
17	118.80	131.843	5.1567	-13.0432	-0.53679	
18	208.70	201.380	7.3022	7.3204	0.30833	
19	173.10	182.749	8.7667	-9.6493	-0.41518	
20	52.40	72.913	10.3353	-20.5129	-0.90815	
21	35.10	53.102	9.9866	-18.0021	-0.79151	
22	36.60	38.051	11.8832	-1.4506	-0.06650	
23	69.30	92.108	8.8122	-22.8082	-0.98209	
24	67.30	89.171	7.3136	-21.8711	-0.92132	
25	178.40	162.676	8.4334	15.7241	0.67299	
26	132.70	129.058	8.4835	3.6421	0.15600	
27	125.00	141.102	11.9953	-16.1016	-0.74025	

28	158.70	125.439	6.6652	33.2612	1.39000	
29	217.30	207.655	11.9741	9.6452	0.44319	
30	208.70	188.834	8.3621	19.8657	0.84932	
31	209.60	187.011	12.1336	22.5887	1.04217	
32	126.00	137.646	9.4269	-11.6455	-0.50673	
33	144.70	97.000	10.8000	47.7003	2.13241	R
34	143.30	122.886	7.6530	20.4144	0.86386	

R denotes an observation with a large standardized residual.

General Regression Analysis: UCS

Regression Equation

UCS = 148.503 + 41.7183 Z1 + 10.6818 Z2 + 14.3758 Z3 + 15.2422 Z4

Summary of Model

S = 24.8399 R-Sq = 80.99% R-Sq(adj) = 78.36%
PRESS = 25726.6 R-Sq(pred) = 72.66%

Analysis of Variance

Source	DF	Seq SS	Adj SS	Adj MS	F	P
Regression	4	76213.2	76213.2	19053.3	30.8797	0.0000000
Z1	1	63606.9	47749.3	47749.3	77.3871	0.0000000
Z3	1	764.6	3292.5	3292.5	5.3361	0.0282026
Z4	1	5359.3	6142.7	6142.7	9.9554	0.0037196
Z6	1	6482.3	6482.3	6482.3	10.5059	0.0029856
Error	29	17893.5	17893.5	617.0		
Total	33	94106.7				

Fits and Diagnostics for All Observations

Obs	UCS	Fit	SE Fit	Residual	St Resid	
1	150.70	135.398	8.8533	15.3023	0.65934	
2	134.60	153.410	7.2085	-18.8103	-0.79132	
3	128.40	170.545	10.1987	-42.1453	-1.86075	
4	153.00	173.661	9.2703	-20.6607	-0.89653	
5	132.70	122.551	7.3618	10.1489	0.42779	
6	125.03	159.440	13.4774	-34.4098	-1.64911	
7	149.60	147.186	11.2062	2.4144	0.10891	
8	120.40	95.952	9.3037	24.4480	1.06149	
9	244.90	235.971	10.1145	8.9286	0.39355	
10	171.40	171.432	9.6161	-0.0318	-0.00139	
11	222.00	189.671	9.3408	32.3285	1.40457	
12	216.52	218.537	9.5248	-2.0166	-0.08791	
13	167.80	226.816	10.2387	-59.0162	-2.60769	R
14	198.94	172.098	9.1979	26.8421	1.16330	
15	192.30	174.288	10.0339	18.0118	0.79267	
16	135.10	141.512	7.8920	-6.4115	-0.27222	
17	118.80	131.843	5.1567	-13.0432	-0.53679	
18	208.70	201.380	7.3022	7.3204	0.30833	
19	173.10	182.749	8.7667	-9.6493	-0.41518	
20	52.40	72.913	10.3353	-20.5129	-0.90815	
21	35.10	53.102	9.9866	-18.0021	-0.79151	
22	36.60	38.051	11.8832	-1.4506	-0.06650	
23	69.30	92.108	8.8122	-22.8082	-0.98209	
24	67.30	89.171	7.3136	-21.8711	-0.92132	
25	178.40	162.676	8.4334	15.7241	0.67299	
26	132.70	129.058	8.4835	3.6421	0.15600	
27	125.00	141.102	11.9953	-16.1016	-0.74025	
28	158.70	125.439	6.6652	33.2612	1.39000	
29	217.30	207.655	11.9741	9.6452	0.44319	
30	208.70	188.834	8.3621	19.8657	0.84932	
31	209.60	187.011	12.1336	22.5887	1.04217	
32	126.00	137.646	9.4269	-11.6455	-0.50673	
33	144.70	97.000	10.8000	47.7003	2.13241	R
34	143.30	122.886	7.6530	20.4144	0.86386	

Appendix B TSR Data

TSR Data N2-3

	Conditioned Samples			Unconditioned Samples		
Sample Number	N2-3-2	N2-3-3	N2-3-7	N2-3-5	N2-3-6	N2-3-8
(A) Diameter, in	5.908	5.911	5.663	5.912	5.910	5.907
(B) Height, in	3.714	3.714	3.715	3.720	3.713	3.733
(C) Weight in Air, gm	3784.5	3782.2	3785.0	3782.2	3786.0	3782.7
(E) Submerged Weight, gm	2158.2	2152.5	2151.7	2152.0	2156.5	2154.1
(D) SSD Weight, gm	3796.0	3794.0	3797.2	3793.9	3797.6	3798.5
(F) Bulk Specific Gravity [C/(D-E)]	2.311	2.304	2.300	2.304	2.307	2.300
(G) Theoretical Maximum Gravity	2.485	2.485	2.485	2.485	2.485	2.485
(H) % Air Voids [100*(1-F/G)]	7.0	7.3	7.4	7.3	7.2	7.4
(I) Volume of Air Voids [H*(D-E)/100]	114.862	119.488	122.361	119.888	117.559	122.187
Calculated Weight Range For 70-80% Saturation						
Weight for 70%	3864.9	3865.8	3870.7	N / A		
Weight for 80%	3876.4	3877.8	3882.9			
If With-in Calculated Range						
(M) SSD Weight, gm	3873.1	3876.5	3881.9	N / A		
(N) Vol. Of Absorbed Water, cc [M - C]	88.6	94.3	96.9			
(O) % Saturation [100*(N/I)]	77.1	78.9	79.2			
Tensile Strength (S_T) Calculations						
(P) Failure Load, lbs	5810	4890	4795	5190	5380	5050
(Q) Dry S_T, psi [2P/(A*B*π)]	N/A	N/A	N/A	150.2	156.1	145.8
(R) Conditioned S_T, psi [2P/(A*B*JI)]	168.6	141.8	145.1	N/A	N/A	N/A
(S) Average S_T, psi	151.8			150.7		
Tensile Strength Ratio [Avg Conditioned S_T / Avg Dry S_T]:	1.01					
Deformation, 0.01 inch						

TSR Data N7-1

	Conditioned Samples			Unconditioned Samples		
Sample Number	N7-1-4	N7-1-5	N7-1-6	N7-1-8	N7-1-9	N7-1-10
(A) Diameter, in	5.903	5.907	5.903	5.905	5.904	5.904
(B) Height, in	3.722	3.722	3.724	3.723	3.721	3.727
(C) Weight in Air, gm	3781.3	3781.7	3778.9	3779.7	3784.3	3780.6
(E) Submerged Weight, gm	2139.2	2138.7	2135.6	2135.3	2139.7	2137.5
(D) SSD Weight, gm	3787.3	3788.7	3785.5	3785.3	3790.0	3786.5
(F) Bulk Specific Gravity [C/(D-E)]	2.294	2.292	2.290	2.291	2.293	2.293
(G) Theoretical Maximum Gravity	2.468	2.468	2.468	2.468	2.468	2.468
(H) % Air Voids [100*(1-F/G)]	7.0	7.1	7.2	7.2	7.1	7.1
(I) Volume of Air Voids [H*(D-E)/100]	115.969	117.707	118.741	118.517	116.953	117.152
Calculated Weight Range For 70-80% Saturation						
Weight for 70%	3862.5	3864.1	3862.0	N / A		
Weight for 80%	3874.1	3875.9	3873.9			
If With-in Calculated Range						
(M) SSD Weight, gm	3863.0	3870.3	3868.2	N / A		
(N) Vol. Of Absorbed Water, cc [M - C]	81.7	88.6	89.3			
(O) % Saturation [100*(N/I)]	70.5	75.3	75.2			
Tensile Strength (S_T) Calculations						
(P) Failure Load, lbs	7050	6450	6910	7260	7740	8010
(Q) Dry S_T, psi [2P/(A*B*π)]	N/A	N/A	N/A	210.2	224.3	231.7
(R) Conditioned S_T, psi [2P/(A*B*π)]	204.3	186.8	200.1	N/A	N/A	N/A
(S) Average S_T, psi	197.1			222.1		
Tensile Strength Ratio [Avg Conditioned S_T / Avg Dry S_T]:				0.89		
Deformation, 0.01 inch						

TSR Data N7-3

	Conditioned Samples			Unconditioned Samples		
Sample Number	N7-3-6	N7-3-7	N7-3-8	N7-3-9	N7-3-10	N7-3-11
(A) Diameter, in	5.910	5.908	5.907	5.909	5.905	5.909
(B) Height, in	3.721	3.718	3.717	3.716	3.719	3.713
(C) Weight in Air, gm	3902.2	3902.8	3899.6	3898.8	3900.8	3897.5
(E) Submerged Weight, gm	2256.2	2260.3	2255.1	2250.5	2254.1	2255.4
(D) SSD Weight, gm	3908.0	3907.8	3904.4	3902.1	3904.5	3902.9
(F) Bulk Specific Gravity [C/(D-E)]	2.362	2.369	2.364	2.361	2.364	2.366
(G) Theoretical Maximum Gravity	2.545	2.545	2.545	2.545	2.545	2.545
(H) % Air Voids [100*(1-F/G)]	7.2	6.9	7.1	7.2	7.1	7.0
(I) Volume of Air Voids [H*(D-E)/100]	118.519	113.983	117.041	119.655	117.669	116.066
Calculated Weight Range For 70-80% Saturation						
Weight for 70%	3985.2	3982.6	3981.5	N / A		
Weight for 80%	3997.0	3994.0	3993.2			
If With-in Calculated Range						
(M) SSD Weight, gm	3985.3	3991.5	3986.3	N / A		
(N) Vol. Of Absorbed Water, cc [M - C]	83.1	88.7	86.7			
(O) % Saturation [100*(N/I)]	70.1	77.8	74.1			
Tensile Strength (S_T) Calculations						
(P) Failure Load, lbs	7300	6575	7700	7600	9000	7980
(Q) Dry S_T, psi [2P/(A*B*π)]	N/A	N/A	N/A	220.3	260.9	231.5
(R) Conditioned S_T, psi [2P/(A*B*JI)]	211.3	190.6	223.3	N/A	N/A	N/A
(S) Average S_T, psi	208.4			237.6		
Tensile Strength Ratio [Avg Conditioned S_T / Avg Dry S_T]:				0.88		
Deformation, 0.01 inch						

TSR Data N8-1

	Conditioned Samples			Unconditioned Samples		
Sample Number	N8-1-5	N8-1-6	N8-1-7	N8-1-9	N8-1-10	N8-1-11
(A) Diameter, in	5.905	5.915	5.908	5.910	5.914	5.910
(B) Height, in	3.719	3.713	3.717	3.725	3.719	3.721
(C) Weight in Air, gm	3662.0	3653.4	3659.9	3661.0	3661.2	3659.3
(E) Submerged Weight, gm	2093.9	2095.9	2088.8	2095.8	2094.2	2091.7
(D) SSD Weight, gm	3696.0	3693.8	3689.1	3697.6	3694.8	3691.5
(F) Bulk Specific Gravity [C/(D-E)]	2.286	2.286	2.287	2.286	2.287	2.287
(G) Theoretical Maximum Gravity	2.456	2.456	2.456	2.456	2.456	2.456
(H) % Air Voids [100*(1-F/G)]	6.9	6.9	6.9	6.9	6.9	6.9
(I) Volume of Air Voids [H*(D-E)/100]	111.058	110.359	110.113	111.165	109.883	109.857
Calculated Weight Range For 70-80% Saturation						
Weight for 70%	3739.7	3730.7	3737.0	N / A		
Weight for 80%	3750.8	3741.7	3748.0			
If With-in Calculated Range						
(M) SSD Weight, gm	3740.7	3735.9	3742.0	N / A		
(N) Vol. Of Absorbed Water, cc [M - C]	78.7	82.5	82.1			
(O) % Saturation [100*(N/I)]	70.9	74.8	74.6			
Tensile Strength (S_T) Calculations						
(P) Failure Load, lbs	3140	2910	3030	3650	3640	3660
(Q) Dry S_T, psi [2P/(A*B*π)]	N/A	N/A	N/A	105.6	105.4	106.0
(R) Conditioned S_T, psi [2P/(A*B*π)]	91.0	84.4	87.8	N/A	N/A	N/A
(S) Average S_T, psi	87.7			105.6		
Tensile Strength Ratio [Avg Conditioned S_T / Avg Dry S_T]:				0.83		
Deformation, 0.01 inch						

TSR Data N8-2

	Conditioned Samples			Unconditioned Samples		
Sample Number	N8-2-1	N8-2-3	N8-2-4	N8-2-5	N8-2-7	N8-2-8
(A) Diameter, in	5.905	5.914	5.910	5.910	5.910	5.913
(B) Height, in	3.719	3.726	3.722	3.723	3.722	3.724
(C) Weight in Air, gm	3856.0	3839.6	3839.0	3840.3	3836.1	3836.3
(E) Submerged Weight, gm	2245.8	2222.4	2218.4	2217.7	2219.3	2217.9
(D) SSD Weight, gm	3872.7	3860.8	3855.8	3855.8	3856.2	3855.2
(F) Bulk Specific Gravity [C/(D-E)]	2.370	2.344	2.345	2.344	2.344	2.343
(G) Theoretical Maximum Gravity	2.534	2.534	2.534	2.534	2.534	2.534
(H) % Air Voids [100*(1-F/G)]	6.5	7.5	7.5	7.5	7.5	7.5
(I) Volume of Air Voids [H*(D-E)/100]	105.195	123.167	122.404	122.591	123.048	123.369
Calculated Weight Range For 70-80% Saturation						
Weight for 70%	3929.6	3925.8	3924.7	N / A		
Weight for 80%	3940.2	3938.1	3936.9			
If With-in Calculated Range						
(M) SSD Weight, gm	3936.7	3927.6	3927.0	N / A		
(N) Vol. Of Absorbed Water, cc [M - C]	80.7	88.0	88.0			
(O) % Saturation [100*(N/I)]	76.7	71.4	71.9			
Tensile Strength (S_T) Calculations						
(P) Failure Load, lbs	5100	4700	4650	5650	5590	5860
(Q) Dry S_T, psi [2P/(A*B*π)]	N/A	N/A	N/A	163.5	161.8	169.4
(R) Conditioned S_T, psi [2P/(A*B*JI)]	147.8	135.8	134.6	N/A	N/A	N/A
(S) Average S_T, psi	139.4			164.9		
Tensile Strength Ratio [Avg Conditioned S_T / Avg Dry S_T]:				0.85		
Deformation, 0.01 inch						

TSR Data N10-1

	Conditioned Samples			Unconditioned Samples		
Sample Number	N10-1-4	N10-1-5	N10-1-6	N10-1-10	N10-1-11	N10-1-12
(A) Diameter, in	5.905	5.906	5.903	5.902	5.903	5.902
(B) Height, in	3.719	3.715	3.718	3.713	3.712	3.712
(C) Weight in Air, gm	3755.5	3758.2	3758.3	3754.7	3756.9	3753.5
(E) Submerged Weight, gm	2117.5	2117.0	2119.4	2114.2	2115.5	2111.8
(D) SSD Weight, gm	3766.7	3768.0	3768.4	3764.0	3764.2	3761.5
(F) Bulk Specific Gravity [C/(D-E)]	2.277	2.276	2.279	2.276	2.279	2.275
(G) Theoretical Maximum Gravity	2.450	2.450	2.450	2.450	2.450	2.450
(H) % Air Voids [100*(1-F/G)]	7.1	7.1	7.0	7.1	7.0	7.1
(I) Volume of Air Voids [H*(D-E)/100]	116.343	117.041	115.000	117.269	115.271	117.659
Calculated Weight Range For 70-80% Saturation						
Weight for 70%	3836.9	3840.1	3838.8	N / A		
Weight for 80%	3848.6	3851.8	3850.3			
If With-in Calculated Range						
(M) SSD Weight, gm	3837.2	3842.9	3846.1	N / A		
(N) Vol. Of Absorbed Water, cc [M - C]	81.7	84.7	87.8			
(O) % Saturation [100*(N/I)]	70.2	72.4	76.3			
Tensile Strength (S_T) Calculations						
(P) Failure Load, lbs	5200	5300	5430	6010	5900	6100
(Q) Dry S_T, psi [2P/(A*B*π)]	N/A	N/A	N/A	174.6	171.4	177.3
(R) Conditioned S_T, psi [2P/(A*B*JI)]	150.7	153.8	157.5	N/A	N/A	N/A
(S) Average S_T, psi	154.0			174.4		
Tensile Strength Ratio [Avg Conditioned S_T / Avg Dry S_T]:				0.88		
Deformation, 0.01 inch						

TSR Data N10-3

	Conditioned Samples			Unconditioned Samples		
Sample Number	N10-3-2	N10-3-3	N10-3-4	N10-3-5	N10-3-6	N10-3-8
(A) Diameter, in	5.910	5.910	5.908	5.910	5.911	5.908
(B) Height, in	3.719	3.716	3.734	3.715	3.715	3.719
(C) Weight in Air, gm	3867.3	3875.3	3876.9	3874.4	3875.3	3875.8
(E) Submerged Weight, gm	2244.0	2241.1	2243.2	2234.9	2242.9	2242.6
(D) SSD Weight, gm	3884.2	3887.2	3891.2	3882.9	3888.7	3888.5
(F) Bulk Specific Gravity [C/(D-E)]	2.358	2.354	2.352	2.351	2.355	2.355
(G) Theoretical Maximum Gravity	2.537	2.537	2.537	2.537	2.537	2.537
(H) % Air Voids [100*(1-F/G)]	7.1	7.2	7.3	7.3	7.2	7.2
(I) Volume of Air Voids [H*(D-E)/100]	115.841	118.587	119.857	120.842	118.287	118.190
Calculated Weight Range For 70-80% Saturation						
Weight for 70%	3948.4	3958.3	3960.8	N / A		
Weight for 80%	3960.0	3970.2	3972.8			
If With-in Calculated Range						
(M) SSD Weight, gm	3958.4	3964.8	3967.6	N / A		
(N) Vol. Of Absorbed Water, cc [M - C]	91.1	89.5	90.7			
(O) % Saturation [100*(N/I)]	78.6	75.5	75.7			
Tensile Strength (S_T) Calculations						
(P) Failure Load, lbs	5495	5960	5940	5660	5400	6310
(Q) Dry S_T, psi [2P/(A*B*π)]	N/A	N/A	N/A	164.1	156.6	182.8
(R) Conditioned S_T, psi [2P/(A*B*Л)]	159.2	172.8	171.4	N/A	N/A	N/A
(S) Average S_T, psi	167.8			167.8		
Tensile Strength Ratio [Avg Conditioned S_T / Avg Dry S_T]:				1.00		
Deformation, 0.01 inch						

TSR Data N11-3

	Conditioned Samples			Unconditioned Samples		
Sample Number	N11-3-2	N11-3-3	N11-3-4	N11-3-5	N11-3-6	N11-3-7
(A) Diameter, in	5.911	5.910	5.911	5.908	5.910	5.910
(B) Height, in	3.721	3.728	3.723	3.725	3.723	3.726
(C) Weight in Air, gm	3873.6	3894.6	3892.0	3893.1	3891.4	3892.6
(E) Submerged Weight, gm	2241.6	2252.1	2249.1	2248.8	2252.5	2251.7
(D) SSD Weight, gm	3886.7	3902.8	3900.2	3900.8	3901.5	3902.3
(F) Bulk Specific Gravity [C/(D-E)]	2.355	2.359	2.357	2.357	2.360	2.358
(G) Theoretical Maximum Gravity	2.544	2.544	2.544	2.544	2.544	2.544
(H) % Air Voids [100*(1-F/G)]	7.4	7.3	7.3	7.4	7.2	7.3
(I) Volume of Air Voids [H*(D-E)/100]	122.458	119.804	121.226	121.693	119.362	120.490
Calculated Weight Range For 70-80% Saturation						
Weight for 70%	3959.3	3978.5	3976.9	N / A		
Weight for 80%	3971.6	3990.4	3989.0			
If With-in Calculated Range						
(M) SSD Weight, gm	3965.8	3979.3	3977.0	N / A		
(N) Vol. Of Absorbed Water, cc [M - C]	92.2	84.7	85.0			
(O) % Saturation [100*(N/I)]	75.3	70.7	70.1			
Tensile Strength (S_T) Calculations						
(P) Failure Load, lbs	4800	5630	5475	6700	6590	6650
(Q) Dry S_T, psi [2P/(A*B*π)]	N/A	N/A	N/A	193.9	190.7	192.3
(R) Conditioned S_T, psi [2P/(A*B*JI)]	138.9	162.7	158.4	N/A	N/A	N/A
(S) Average S_T, psi	153.3			192.3		
Tensile Strength Ratio [Avg Conditioned S_T / Avg Dry S_T]:	0.80					
Deformation, 0.01 inch						

TSR Data N12-1

	Conditioned Samples			Unconditioned Samples		
Sample Number	N12-1-3	N12-1-5	N12-1-8	N12-1-6	N12-1-9	N12-1-12
(A) Diameter, in	5.906	5.904	5.907	5.907	5.904	5.902
(B) Height, in	3.722	3.714	3.716	3.715	3.721	3.719
(C) Weight in Air, gm	3634.7	3633.1	3633.2	3633.9	3632.1	3633.4
(E) Submerged Weight, gm	2065.3	2058.5	2061.3	2060.9	2064.3	2064.5
(D) SSD Weight, gm	3658.5	3655.1	3656.8	3658.1	3657.9	3656.8
(F) Bulk Specific Gravity [C/(D-E)]	2.281	2.276	2.277	2.275	2.279	2.282
(G) Theoretical Maximum Gravity	2.454	2.454	2.454	2.454	2.454	2.454
(H) % Air Voids [100*(1-F/G)]	7.0	7.3	7.2	7.3	7.1	7.0
(I) Volume of Air Voids [H*(D-E)/100]	112.067	116.119	114.978	116.393	113.527	111.697
Calculated Weight Range For 70-80% Saturation						
Weight for 70%	3713.1	3714.4	3713.7	N / A		
Weight for 80%	3724.4	3726.0	3725.2			
If With-in Calculated Range						
(M) SSD Weight, gm	3713.1	3719.1	3720.0	N / A		
(N) Vol. Of Absorbed Water, cc [M - C]	78.4	86.0	86.8			
(O) % Saturation [100*(N/I)]	70.0	74.1	75.5			
Tensile Strength (S_T) Calculations						
(P) Failure Load, lbs	3725	3710	3725	3675	3990	4010
(Q) Dry S_T, psi [2P/(A*B*π)]	N/A	N/A	N/A	106.6	115.6	116.3
(R) Conditioned S_T, psi [2P/(A*B*JI)]	107.9	107.7	108.0	N/A	N/A	N/A
(S) Average S_T, psi	107.9			112.8		
Tensile Strength Ratio [Avg Conditioned S_T / Avg Dry S_T]:				0.96		
Deformation, 0.01 inch						

TSR Data S2-1

	Conditioned Samples			Unconditioned Samples		
Sample Number	S2-1-3	S2-1-4	S2-1-5	S2-1-6	S2-1-8	S2-1-9
(A) Diameter, in	5.904	5.908	5.903	5.905	5.905	5.904
(B) Height, in	3.713	3.723	3.721	3.723	3.725	3.724
(C) Weight in Air, gm	3688.9	3684.3	3688.9	3683.3	3685.6	3687.0
(E) Submerged Weight, gm	2082.0	2082.4	2087.4	2075.8	2092.3	2085.3
(D) SSD Weight, gm	3714.5	3716.0	3716.4	3708.0	3719.8	3716.9
(F) Bulk Specific Gravity [C/(D-E)]	2.260	2.255	2.265	2.257	2.265	2.260
(G) Theoretical Maximum Gravity	2.431	2.431	2.431	2.431	2.431	2.431
(H) % Air Voids [100*(1-F/G)]	7.0	7.2	6.8	7.2	6.8	7.0
(I) Volume of Air Voids [H*(D-E)/100]	115.059	118.051	111.559	117.062	111.416	114.940
Calculated Weight Range For 70-80% Saturation						
Weight for 70%	3769.4	3766.9	3767.0	N / A		
Weight for 80%	3780.9	3778.7	3778.1			
If With-in Calculated Range						
(M) SSD Weight, gm	3774.3	3767.5	3767.5	N / A		
(N) Vol. Of Absorbed Water, cc [M - C]	85.4	83.2	78.6			
(O) % Saturation [100*(N/I)]	74.2	70.5	70.5			
Tensile Strength (S_T) Calculations						
(P) Failure Load, lbs	8300	8700	9050	8625	7813	8938
(Q) Dry S_T, psi [2P/(A*B*π)]	N/A	N/A	N/A	249.8	226.1	258.8
(R) Conditioned S_T, psi [2P/(A*B*JI)]	241.0	251.8	262.3	N/A	N/A	N/A
(S) Average S_T, psi	251.7			244.9		
Tensile Strength Ratio [Avg Conditioned S_T / Avg Dry S_T]:				1.03		
Deformation, 0.01 inch						

TSR Data S6-1

	Conditioned Samples			Unconditioned Samples		
Sample Number	S6-1-2	S6-1-3	S6-1-5	S6-1-7	S6-1-8	S6-1-10
(A) Diameter, in	5.909	5.915	5.912	5.914	5.917	5.915
(B) Height, in	3.726	3.726	3.723	3.723	3.726	3.720
(C) Weight in Air, gm	3748.8	3747.2	3746.0	3748.6	3747.3	3746.3
(E) Submerged Weight, gm	2122.7	2119.9	2120.7	2121.2	2120.7	2124.8
(D) SSD Weight, gm	3756.7	3754.5	3753.3	3755.7	3755.6	3756.8
(F) Bulk Specific Gravity [C/(D-E)]	2.294	2.292	2.294	2.293	2.292	2.296
(G) Theoretical Maximum Gravity	2.467	2.467	2.467	2.467	2.467	2.467
(H) % Air Voids [100*(1-F/G)]	7.0	7.1	7.0	7.0	7.1	7.0
(I) Volume of Air Voids [H*(D-E)/100]	114.422	115.670	114.157	115.003	115.930	113.435
Calculated Weight Range For 70-80% Saturation						
Weight for 70%	3828.9	3828.2	3825.9	N / A		
Weight for 80%	3840.3	3839.7	3837.3			
If With-in Calculated Range						
(M) SSD Weight, gm	3829.4	3835.1	3827.9	N / A		
(N) Vol. Of Absorbed Water, cc [M - C]	80.6	87.9	81.9			
(O) % Saturation [100*(N/I)]	70.4	76.0	71.7			
Tensile Strength (S_T) Calculations						
(P) Failure Load, lbs	5250	4920	5200	5490	6200	6100
(Q) Dry S_T, psi [2P/(A*B*π)]	N/A	N/A	N/A	158.7	179.0	176.5
(R) Conditioned S_T, psi [2P/(A*B*Л)]	151.8	142.1	150.4	N/A	N/A	N/A
(S) Average S_T, psi	148.1			171.4		
Tensile Strength Ratio [Avg Conditioned S_T / Avg Dry S_T]:				0.86		
Deformation, 0.01 inch						

TSR Data S7-1

	Conditioned Samples			Unconditioned Samples		
Sample Number	S7-1-4	S7-1-5	S7-1-6	S7-1-8	S7-1-9	S7-1-10
(A) Diameter, in	5.907	5.903	5.907	5.909	5.910	5.912
(B) Height, in	3.731	3.729	3.727	3.726	3.724	3.735
(C) Weight in Air, gm	3728.8	3731.4	3727.1	3730.8	3729.5	3727.9
(E) Submerged Weight, gm	2130.5	2122.2	2114.8	2130.3	2124.6	2121.8
(D) SSD Weight, gm	3762.1	3755.7	3750.7	3763.4	3758.5	3755.4
(F) Bulk Specific Gravity [C/(D-E)]	2.285	2.284	2.278	2.284	2.283	2.282
(G) Theoretical Maximum Gravity	2.454	2.454	2.454	2.454	2.454	2.454
(H) % Air Voids [100*(1-F/G)]	6.9	6.9	7.2	6.9	7.0	7.0
(I) Volume of Air Voids [H*(D-E)/100]	112.122	112.962	117.114	112.807	114.136	114.488
Calculated Weight Range For 70-80% Saturation						
Weight for 70%	3807.3	3810.5	3809.1	N / A		
Weight for 80%	3818.5	3821.8	3820.8			
If With-in Calculated Range						
(M) SSD Weight, gm	3809.7	3812.5	3812.2	N / A		
(N) Vol. Of Absorbed Water, cc [M - C]	80.9	81.1	85.1			
(O) % Saturation [100*(N/I)]	72.2	71.8	72.7			
Tensile Strength (S_T) Calculations						
(P) Failure Load, lbs	7260	6940	6900	7760	7820	7470
(Q) Dry S_T, psi [2P/(A*B*π)]	N/A	N/A	N/A	224.4	226.2	215.4
(R) Conditioned S_T, psi [2P/(A*B*Л)]	209.7	200.7	199.5	N/A	N/A	N/A
(S) Average S_T, psi	203.3			222.0		
Tensile Strength Ratio [Avg Conditioned S_T / Avg Dry S_T]:				0.92		
Deformation, 0.01 inch						

TSR Data S8-2

	Conditioned Samples			Unconditioned Samples		
Sample Number	S8-2-3	S8-2-4	S8-2-7	S8-2-5	S8-2-6	S8-2-8
(A) Diameter, in	5.917	5.916	5.905	5.910	5.908	5.908
(B) Height, in	3.716	3.718	3.712	3.711	3.714	3.716
(C) Weight in Air, gm	3864.4	3864.5	3865.3	3861.6	3859.6	3861.5
(E) Submerged Weight, gm	2229.1	2235.2	2221.9	2231.0	2231.6	2230.0
(D) SSD Weight, gm	3877.6	3877.3	3872.0	3875.0	3873.0	3873.8
(F) Bulk Specific Gravity [C/(D-E)]	2.344	2.353	2.342	2.349	2.351	2.349
(G) Theoretical Maximum Gravity	2.532	2.532	2.532	2.532	2.532	2.532
(H) % Air Voids [100*(1-F/G)]	7.4	7.1	7.5	7.2	7.1	7.2
(I) Volume of Air Voids [H*(D-E)/100]	122.276	115.836	123.520	118.882	117.071	118.721
Calculated Weight Range For 70-80% Saturation						
Weight for 70%	3950.0	3945.6	3951.8	N / A		
Weight for 80%	3962.2	3957.2	3964.1			
If With-in Calculated Range						
(M) SSD Weight, gm	3957.0	3953.2	3954.0	N / A		
(N) Vol. Of Absorbed Water, cc [M - C]	92.6	88.7	88.7			
(O) % Saturation [100*(N/I)]	75.7	76.6	71.8			
Tensile Strength (S_T) Calculations						
(P) Failure Load, lbs	4625	4725	4910	4990	4880	4790
(Q) Dry S_T, psi [2P/(A*B*π)]	N/A	N/A	N/A	144.8	141.6	138.9
(R) Conditioned S_T, psi [2P/(A*B*π)]	133.9	136.8	142.6	N/A	N/A	N/A
(S) Average S_T, psi	137.8			141.8		
Tensile Strength Ratio [Avg Conditioned S_T / Avg Dry S_T]:				0.97		
Deformation, 0.01 inch						

TSR Data S8-3

	Conditioned Samples			Unconditioned Samples		
Sample Number	S8-3-5	S8-3-4	S8-3-7	S8-3-11	S8-3-13	S8-3-14
(A) Diameter, in	5.911	5.906	5.910	5.910	5.914	5.909
(B) Height, in	3.712	3.726	3.717	3.717	3.716	3.715
(C) Weight in Air, gm	3878.0	3874.8	3875.1	3875.7	3872.4	3870.7
(E) Submerged Weight, gm	2242.3	2231.8	2239.7	2237.1	2239.6	2240.8
(D) SSD Weight, gm	3887.4	3883.7	3885.3	3884.3	3884.0	3882.2
(F) Bulk Specific Gravity [C/(D-E)]	2.357	2.346	2.355	2.353	2.355	2.358
(G) Theoretical Maximum Gravity	2.532	2.532	2.532	2.532	2.532	2.532
(H) % Air Voids [100*(1-F/G)]	6.9	7.4	7.0	7.1	7.0	6.9
(I) Volume of Air Voids [H*(D-E)/100]	113.504	121.568	115.150	116.513	115.016	112.688
Calculated Weight Range For 70-80% Saturation						
Weight for 70%	3957.5	3959.9	3955.7	N / A		
Weight for 80%	3968.8	3972.1	3967.2			
If With-in Calculated Range						
(M) SSD Weight, gm	3964.6	3960.4	3957.8	N / A		
(N) Vol. Of Absorbed Water, cc [M - C]	86.6	85.6	82.7			
(O) % Saturation [100*(N/I)]	76.3	70.4	71.8			
Tensile Strength (S_T) Calculations						
(P) Failure Load, lbs	4150	3500	4375	4880	4525	4525
(Q) Dry S_T, psi [2P/(A*B*π)]	N/A	N/A	N/A	141.4	131.1	131.2
(R) Conditioned S_T, psi [2P/(A*B*Л)]	120.4	101.3	126.8	N/A	N/A	N/A
(S) Average S_T, psi	116.2			134.6		
Tensile Strength Ratio [Avg Conditioned S_T / Avg Dry S_T]:				0.86		
Deformation, 0.01 inch						

TSR Data S10-2

	Conditioned Samples			Unconditioned Samples		
Sample Number	S10-2-2	S10-2-3	S10-2-4	S10-2-5	S10-2-6	S10-2-7
(A) Diameter, in	5.906	5.908	5.909	5.909	5.907	5.907
(B) Height, in	3.721	3.718	3.721	3.720	3.724	3.718
(C) Weight in Air, gm	3937.2	3909.8	3913.8	3914.7	3912.4	3915.1
(E) Submerged Weight, gm	2297.0	2274.4	2272.7	2279.0	2281.0	2273.7
(D) SSD Weight, gm	3948.7	3919.8	3921.7	3926.9	3923.2	3923.0
(F) Bulk Specific Gravity [C/(D-E)]	2.384	2.376	2.373	2.376	2.382	2.374
(G) Theoretical Maximum Gravity	2.550	2.550	2.550	2.550	2.550	2.550
(H) % Air Voids [100*(1-F/G)]	6.5	6.8	6.9	6.8	6.6	6.9
(I) Volume of Air Voids [H*(D-E)/100]	107.700	112.145	114.176	112.724	107.925	113.967
Calculated Weight Range For 70-80% Saturation						
Weight for 70%	4012.6	3988.3	3993.7	N / A		
Weight for 80%	4023.4	3999.5	4005.1			
If With-in Calculated Range						
(M) SSD Weight, gm	4012.6	3996.2	4000.6	N / A		
(N) Vol. Of Absorbed Water, cc [M - C]	75.4	86.4	86.8			
(O) % Saturation [100*(N/I)]	70.0	77.0	76.0			
Tensile Strength (S_T) Calculations						
(P) Failure Load, lbs	4600	4400	4400	5000	5350	5500
(Q) Dry S_T, psi [2P/(A*B*π)]	N/A	N/A	N/A	144.8	154.8	159.4
(R) Conditioned S_T, psi [2P/(A*B*JI)]	133.3	127.5	127.4	N/A	N/A	N/A
(S) Average S_T, psi	129.4			153.0		
Tensile Strength Ratio [Avg Conditioned S_T / Avg Dry S_T]:				0.85		
Deformation, 0.01 inch						

TSR Data S10-3

	Conditioned Samples			Unconditioned Samples		
Sample Number	S10-3-3	S10-3-4	S10-3-5	S10-3-6	S10-3-7	S10-3-8
(A) Diameter, in	5.906	5.908	5.906	5.906	5.912	5.913
(B) Height, in	3.723	3.719	3.721	3.716	3.718	3.721
(C) Weight in Air, gm	3907.2	3906.0	3910.3	3909.1	3911.1	3906.5
(E) Submerged Weight, gm	2263.3	2264.7	2269.9	2264.1	2274.7	2264.5
(D) SSD Weight, gm	3912.9	3914.6	3918.9	3916.0	3921.5	3913.9
(F) Bulk Specific Gravity [C/(D-E)]	2.369	2.367	2.371	2.366	2.375	2.368
(G) Theoretical Maximum Gravity	2.553	2.553	2.553	2.553	2.553	2.553
(H) % Air Voids [100*(1-F/G)]	7.2	7.3	7.1	7.3	7.0	7.2
(I) Volume of Air Voids [H*(D-E)/100]	119.165	119.935	117.351	120.721	114.838	119.239
Calculated Weight Range For 70-80% Saturation						
Weight for 70%	3990.6	3990.0	3992.4	N / A		
Weight for 80%	4002.5	4001.9	4004.2			
If With-in Calculated Range						
(M) SSD Weight, gm	3991.3	4000.2	3999.4	N / A		
(N) Vol. Of Absorbed Water, cc [M - C]	84.1	94.2	89.1			
(O) % Saturation [100*(N/I)]	70.6	78.5	75.9			
Tensile Strength (S_T) Calculations						
(P) Failure Load, lbs	3910	3600	3675	4490	4600	4650
(Q) Dry S_T, psi [2P/(A*B*π)]	N/A	N/A	N/A	130.3	133.2	134.6
(R) Conditioned S_T, psi [2P/(A*B*JI)]	113.2	104.3	106.5	N/A	N/A	N/A
(S) Average S_T, psi	108.0			132.7		
Tensile Strength Ratio [Avg Conditioned S_T / Avg Dry S_T]:				0.81		
Deformation, 0.01 inch						

TSR Data S11-2

	Conditioned Samples			Unconditioned Samples		
Sample Number	S11-2-3	S11-2-4	S11-2-5	S11-2-1	S11-2-6	S11-2-8
(A) Diameter, in	5.915	5.913	5.910	5.915	5.915	5.914
(B) Height, in	3.723	3.722	3.722	3.718	3.722	3.713
(C) Weight in Air, gm	3907.0	3905.8	3907.9	3887.4	3906.0	3905.8
(E) Submerged Weight, gm	2279.7	2275.7	2270.5	2259.1	2274.6	2282.2
(D) SSD Weight, gm	3921.7	3918.1	3917.1	3902.7	3919.6	3922.6
(F) Bulk Specific Gravity [C/(D-E)]	2.379	2.378	2.373	2.365	2.374	2.381
(G) Theoretical Maximum Gravity	2.555	2.555	2.555	2.555	2.555	2.555
(H) % Air Voids [100*(1-F/G)]	6.9	6.9	7.1	7.4	7.1	6.8
(I) Volume of Air Voids [H*(D-E)/100]	112.841	113.711	117.089	122.113	116.233	111.711
Calculated Weight Range For 70-80% Saturation						
Weight for 70%	3986.0	3985.4	3989.9	N / A		
Weight for 80%	3997.3	3996.8	4001.6			
If With-in Calculated Range						
(M) SSD Weight, gm	3993.1	3991.9	3993.5	N / A		
(N) Vol. Of Absorbed Water, cc [M - C]	86.1	86.1	85.6			
(O) % Saturation [100*(N/I)]	76.3	75.7	73.1			
Tensile Strength (S_T) Calculations						
(P) Failure Load, lbs	4580	4580	4900	4900	5400	5200
(Q) Dry S_T, psi [2P/(A*B*π)]	N/A	N/A	N/A	141.8	156.2	150.8
(R) Conditioned S_T, psi [2P/(A*B*JI)]	132.4	132.5	141.8	N/A	N/A	N/A
(S) Average S_T, psi	135.6			149.6		
Tensile Strength Ratio [Avg Conditioned S_T / Avg Dry S_T]:				0.91		
Deformation, 0.01 inch						

TSR Data S11-3

	Conditioned Samples			Unconditioned Samples		
Sample Number	S11-3-2	S11-3-3	S11-3-4	S11-3-5	S11-3-6	S11-3-7
(A) Diameter, in	5.912	5.918	5.917	5.917	5.915	5.913
(B) Height, in	3.715	3.724	3.718	3.720	3.718	3.728
(C) Weight in Air, gm	3887.3	3868.2	3864.9	3866.3	3870.3	3907.0
(E) Submerged Weight, gm	2243.5	2220.3	2225.5	2228.9	2225.3	2255.5
(D) SSD Weight, gm	3893.0	3874.4	3874.5	3876.8	3875.4	3915.4
(F) Bulk Specific Gravity [C/(D-E)]	2.357	2.339	2.344	2.346	2.345	2.354
(G) Theoretical Maximum Gravity	2.522	2.522	2.522	2.522	2.522	2.522
(H) % Air Voids [100*(1-F/G)]	6.6	7.3	7.1	7.0	7.0	6.7
(I) Volume of Air Voids [H*(D-E)/100]	108.144	120.317	116.526	114.871	115.485	110.733
Calculated Weight Range For 70-80% Saturation						
Weight for 70%	3963.0	3952.4	3946.5	N / A		
Weight for 80%	3973.8	3964.5	3958.1			
If With-in Calculated Range						
(M) SSD Weight, gm	3970.6	3952.7	3957.0	N / A		
(N) Vol. Of Absorbed Water, cc [M - C]	83.3	84.5	92.1			
(O) % Saturation [100*(N/I)]	77.0	70.2	79.0			
Tensile Strength (S_T) Calculations						
(P) Failure Load, lbs	3560	3420	3275	3890	4200	4400
(Q) Dry S_T, psi [2P/(A*B*π)]	N/A	N/A	N/A	112.5	121.6	127.1
(R) Conditioned S_T, psi [2P/(A*B*Л)]	103.2	98.8	94.8	N/A	N/A	N/A
(S) Average S_T, psi	98.9			120.4		
Tensile Strength Ratio [Avg Conditioned S_T / Avg Dry S_T]:				0.82		
Deformation, 0.01 inch						

TSR Data S12-1

	Conditioned Samples			Unconditioned Samples		
Sample Number	S12-1-3	S12-1-4	S12-1-8	S12-1-5	S12-1-6	S12-1-7
(A) Diameter, in	5.907	5.905	5.915	5.908	5.913	5.912
(B) Height, in	3.727	3.723	3.734	3.721	3.724	3.726
(C) Weight in Air, gm	3805.4	3808.0	3807.1	3805.2	3805.1	3805.2
(E) Submerged Weight, gm	2160.0	2160.0	2155.7	2158.0	2158.0	2156.4
(D) SSD Weight, gm	3813.8	3813.9	3813.5	3811.9	3812.9	3811.5
(F) Bulk Specific Gravity [C/(D-E)]	2.301	2.302	2.296	2.301	2.299	2.299
(G) Theoretical Maximum Gravity	2.473	2.473	2.473	2.473	2.473	2.473
(H) % Air Voids [100*(1-F/G)]	7.0	6.9	7.1	7.0	7.0	7.0
(I) Volume of Air Voids [H*(D-E)/100]	115.021	114.070	118.334	115.202	116.242	116.402
Calculated Weight Range For 70-80% Saturation						
Weight for 70%	3885.9	3887.8	3889.9	N / A		
Weight for 80%	3897.4	3899.3	3901.8			
If With-in Calculated Range						
(M) SSD Weight, gm	3886.8	3893.9	3895.1	N / A		
(N) Vol. Of Absorbed Water, cc [M - C]	81.4	85.9	88.0			
(O) % Saturation [100*(N/I)]	70.8	75.3	74.4			
Tensile Strength (S_T) Calculations						
(P) Failure Load, lbs	4920	5020	5130	5790	5800	6700
(Q) Dry S_T, psi [2P/(A*B*π)]	N/A	N/A	N/A	167.7	167.7	193.6
(R) Conditioned S_T, psi [2P/(A*B*π)]	142.3	145.4	147.9	N/A	N/A	N/A
(S) Average S_T, psi	145.2			176.3		
Tensile Strength Ratio [Avg Conditioned S_T / Avg Dry S_T]:				0.82		
Deformation, 0.01 inch						

TSR Data S12-3

	Conditioned Samples			Unconditioned Samples		
Sample Number	S12-3-3	S12-3-4	S12-3-5	S12-3-6	S12-3-8	S12-3-9
(A) Diameter, in	5.904	5.902	5.900	5.904	5.906	5.903
(B) Height, in	3.719	3.719	3.715	3.712	3.715	3.719
(C) Weight in Air, gm	3886.8	3886.4	3886.2	3886.0	3885.4	3883.6
(E) Submerged Weight, gm	2250.1	2244.1	2247.7	2247.5	2244.8	2251.9
(D) SSD Weight, gm	3896.1	3894.7	3894.8	3895.8	3893.9	3896.2
(F) Bulk Specific Gravity [C/(D-E)]	2.361	2.355	2.359	2.358	2.356	2.362
(G) Theoretical Maximum Gravity	2.533	2.533	2.533	2.533	2.533	2.533
(H) % Air Voids [100*(1-F/G)]	6.8	7.0	6.9	6.9	7.0	6.8
(I) Volume of Air Voids [H*(D-E)/100]	111.535	116.293	112.872	114.151	115.188	111.098
Calculated Weight Range For 70-80% Saturation						
Weight for 70%	3964.9	3967.8	3965.2	N / A		
Weight for 80%	3976.0	3979.4	3976.5			
If With-in Calculated Range						
(M) SSD Weight, gm	3967.0	3971.6	3973.0	N / A		
(N) Vol. Of Absorbed Water, cc [M - C]	80.2	85.2	86.8			
(O) % Saturation [100*(N/I)]	71.9	73.3	76.9			
Tensile Strength (S_T) Calculations						
(P) Failure Load, lbs	6100	6050	5800	5900	5100	6100
(Q) Dry S_T, psi [2P/(A*B*π)]	N/A	N/A	N/A	171.4	148.0	176.9
(R) Conditioned S_T, psi [2P/(A*B*JI)]	176.9	175.5	168.5	N/A	N/A	N/A
(S) Average S_T, psi	173.6			165.4		
Tensile Strength Ratio [Avg Conditioned S_T / Avg Dry S_T]:	1.05					
Deformation, 0.01 inch						